From the
Medizinischen Klinik und Poliklinik I Großhadern
of the Ludwig-Maximilians-Universität München
Direktor: Prof. Dr. med. Steffen Massberg

The role of leukocyte-megakaryocyte interactions during the thrombopoiesis

Dissertation
zum Erwerb des Doctor of Philosophy (Ph.D.) an der
Medizinischen Fakultät der Ludwig-Maximilians-Universität

submitted by Zhe Zhang

20.05.2019

Supervisor(s): Prof. Dr. med. Steffen Massberg

Second expert: Prof. Dr. med. Steffen Massberg

Dean: Prof. Dr. med. dent. Reinhard Hickel

Date of oral defense: 20.07.2020

Table of contents

.

Abbreviation

ACD	Acid citrate dextrose
ANOVA	Analysis of variance
BSA	Bovine serum albumin
CD	Cluster of differentiation
Cre	Causes recombination
CXCR	C-X-C chemokine receptor
CXCL	C-X-C Chemokine Ligand
DT	Diphtheria toxin
eYFP	Enhanced yellow fluorescent protein
eGFP	Enhanced green fluorescent protein
FACS	Fluorescence activated cell sorting
Flox	Flanked by loxP sites
ICAM-1	Intercellular cell adhesion molecule-1
iDTR	Inducible Diphtheria toxin receptor
Ig	Immunoglobulins
LFA-1	Leukocyte function-associated antigen-1
mTPO	Mouse thrombopoietin
MK	Megakaryocyte
MP-IVM	Multiphoton-intravital microscopy
NA	Numerical aperture
NET	Neutrophil extracellular traps
OPO	Optical parametric oscillator

PAF	Proplatelet associated fragment
PBS	Phosphate buffered saline
PFA	Paraformaldehyde
PMA	Phorbol myristate acetate
PMN	Polymorphonuclear neutrophils
PPF	Proplatelet forming
ROS	Reactive oxygen species
SEM	Standard error of the mean
SDF-1	Stromal cell-derived factor 1
S1P	Sphingosine 1-phosphate
TO	Thiazole orange
Ti:sa	Ti: sapphire
WT	Wild type
WBC	White blood cells
vWF	Von Willebrand factor
ZT	Zeitgeber time

List of figures

List of tables

Abstract

Platelets are small-sized, anucleated cells with a lifespan of 5-8 days that circulate within the blood to maintain vessel integrity and to prevent bleeding after injury in mammals. Beyond its classical roles，platelets are further involved in a variety of physiological and pathological processes, like inflammation, immune defensing, cancer metastasis, and etc. Each day approximately 15×10^9 to 40×10^9 platelets are continuously released into the circulation by their progenitors, megakaryocytes (MK). MKs represent only 0.01% of bone marrow (BM) cells, however are able to release several hundred platelets by fragmentation from one MK into the circulation by a process termed thrombopoiesis. This process goes along with the formation of proplatelets, long cell body extensions, which are shedded off. However, these precise molecular underlying mechanisms are still largely unknown and only few factors, like shear stress or S1P, have been identified to affect this process. In particular, the role of other cell types in this process remains elusive, considering close proximity of various immune cells with MKs within the bone marrow. Herein, we evaluated platelet production in the presence or absence of neutrophils. Our data indicates neutrophils augment platelet counts by increasing the reticulated platelet biogenesis. Using multiphoton intravital microscopy we observed PMN-MK interactions within the interstitium and vasculature niches. Our data shows neutrophils in circulation pool dominate proplatelet forming and shedding. In addition, using genetic mice in an in vitro co-culture assay, we identified the role of CXCR4/SDF-1 and reactive oxygen species (ROS) in thrombopoiesis. To do so, we found that these observed mechanisms contribute to the diurnal modulation of platelet counts of the day. Taken together, we identified PMN-MK interaction within the bone marrow as regulator of thrombopoiesis.

2. Introduction

2.1 Megakaryocyte development

Megakaryocytes mainly reside in the BM, but could also be found in the yolk sac, fetal liver in the early development stage, spleen and lung of adult animals (Long et al. 1982; Ogawa, 1993; William B. Slayton, et al. 2012; Lefrançais E, et al. 2017). Platelets are primarily released from megakaryocytes that locate within the bone marrow. However, a recent study demonstrated that MKs reside within the lung vasculature and contribute to platelet production (Lefrançais E, et al. 2017). Inside the bone marrow, megakaryocytes derive from a MK biased progenitor cell (MPC). MPCs are derived from haematopoietic stem cell that maintain their self-renewal or differentiation capacities throughout lifetime. Within the BM HSCs are able to differentiate into different blood lineages including the common lymphoid progenitors (CLPs) and common myeloid progenitors (CMPs). Subsequently CMP cells undergo cellular differentiation into the granulocyte/macrophage progenitors or the megakaryocyte-erythrocyte progenitors (Carolien M. Woolthuis, et al. 2016, Haas S, et al. 2015). At later stages, the megakaryocyte-erythrocyte progenitors will further develop into megakaryocytes or erythrocytes under the effects of a series of different chemokines or cytokines, such as IL-3, IL-6, etc. (Broudy VC, et al. 1995; Deutsch VR, et al. 2013; Carolien M. Woolthuis, et al. 2016).

The MK differentiation (termed as Megakaryopoiesis) is primarily regulated by thrombopoietin (TPO) that is capable of binding to its receptor (Mpl) on the cell surface of MKs to maintain constant platelet counts within the blood (Broudy VC, et al. 1995). TPO is primarily produced in the liver and to some extent within the BM and kidney (Sungaran R, et al. 1997; Shinguang Qian, et al. 1998). Within the blood TPO plasma level show an inverse relationship with platelet counts (Nichol et al. 1995; Engel C, et al. 1999). Under steady state

conditions, hepatocyte derived thrombopoietin release can be regulated through a c-MP-mediated hormone uptake and destruction way (Kenneth Kaushansky, 2005). Under inflammatory conditions, macrophages released IL-6 was found to stimulate TPO release (Kaser A, et al. 2001). Few years ago, it was shown that TPO production is regulated through changes of platelet surface sialyation pattern, particular on aged platelets (Renata Grozovsky, et al. 2015). Even though TPO dominates the differentiation of MK maturation, and TPO- and c-Mpl null mice have a severe thrombocytopenia, these mice retain their ability to release proplatelet into bone marrow sinusoids. This finding furthermore elucidates that TPO and c-Mpl play an important role during megakaryopoiesis but not thrombopoiesis (Choi, et al. 1995; Ito, et al. 1996; Solar GP, et al. 1998).

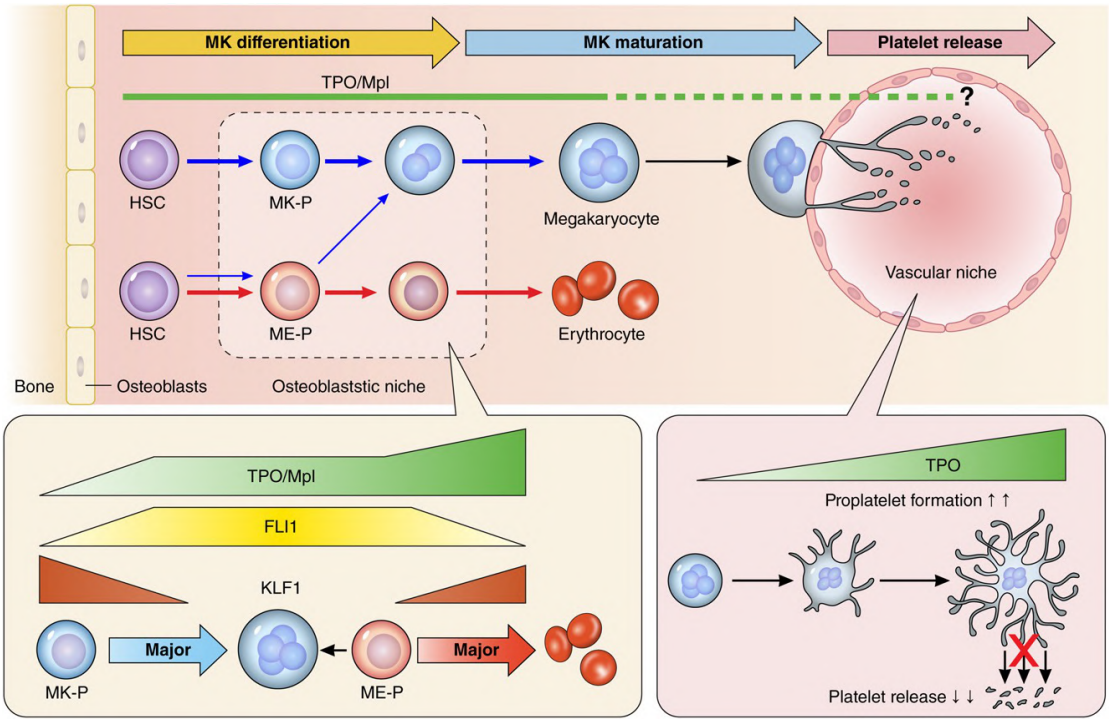

Fig.2.1 Megakaryocyte differentiation (Eto K, Kunishima S. 2016).

During megakaryopoiesis, TPO drives the differentiation of platelet biased hematopoietic stem cells into megakaryocytic progenitors. During their maturation, megakaryocyte undergo a process called endomitosis to yield a polyploid state without undergoing cell division. This kind of endomitosis has been deemed useful to efficiently accumulate the enourmous amounts of proteins and RNAs that are transferred in the forming platelets (Zimmet & Ravid, 2000; Machlus & Italiano, 2013). Megakaryopoiesis is regulated by transcription factors, like GATA-1, friend of GATA-1 (FOG-1), NF-E2, RUNX1, etc. (Crispino, J.D. 2005, Avanzi MP, et al. 2014). From these transcription factors, GATA-1 plays the prominent role as it facilitates the recruitment of chromatin activation and repression elements and other transcription factors, like FOG-1, etc. (Crispino, J.D., 2005). Along this line, GATA-1 deficient mice exhibit a hyperproliferative and thrombocytopenic phenotype underscoring its central role in the megakaryopoiesis (Vyas P, et al. 1999). NF-E2 has also been demonstrated that it could drive the differentiation of MKs and impact on platelet formation through binding to the Maf recognition element and further regulating the maturation stage-specific genes, (Shivdasani RA, et al. 1995; Shavit JA, et al. 1998).

In addition, some stromal cells, like arteriolar cells in the bones, are also deemed as determinant to the development of megakaryocytes, as the arteriolar niche are associated with the distribution of subsets of quiescent HSCs (Kunisaki Y, et al.2013). Initial studies implied that during the maturation process MKs translocate from the osteoblastic niche to perivascular niche. However, this concept was recently challenged that sinusoid MK precursors directly replenished the MK number and their distributions proximately associated with the MK niche rather than the arteriolar niche (Stegner D. et al. 2017; Pinho S, et al. 2018).

2.2 Leukocyte-platelet interaction

Beyond their pivotal role in primary hemostasis, platelets have a variety of functions during inflammation. Under steady state conditions, platelets circulate within the blood in a quiescent state. However, upon activation following vascular injury (e.g. atherothrombosis), platelets undergo a shape change, secret their granular content and conformationally activate surface expressed adhesion molecules (i.e. integrins). The shape change of platelet and the expression of adhesive molecules strongly associated with later stages of platelet-leukocyte and platelet–endothelium interactions that are important for the maintenance of vessel wall integrity and host immune defense.

Platelets communication with leukocytes, mainly neutrophils, by secreting proteins and non-protein molecules, for instance ADP, to intercommunicate with leukocytes. Moreover, leukocytes are able to release factors, including proteases and nitric oxide, to modulate the response of platelets. It has been well-known that the platelet-neutrophil interaction is of essential importance under various pathophysiological conditions, including bacterial infections, sepsis, sickle cell disease, acute lung injury, nocturnal asthma, etc. (Gawaz et al. 1995, Pamuk et al. 2006, Polanowska-Grabowska et al. 2010, Gresele et al. 1993; Caudrillier et al. 2012.). Platelet-neutrophil interactions are mediated through several mechanisms: I) platelets express p-selectin (CD62P) binds to neutrophil expressed P-selectin glycoprotein ligand-1 (Hamburger and McEver 1990; Moore et al. 1995), and II) platelet glycoprotein Ibα binds to MAC-1 on neutrophils (Simon et al. 2000). Under inflammatory conditions, platelets facilitate the adhesion of neutrophils to the activated or injured endothelium cells to promote neutrophil transmigration (Sreeramkumar V, et al. 2014; Gabriele Zuchtriegel, et al. 2016). Neutrophils act as the first responding cell type to tackle invading pathogens, underscoring their crucial role during host

defense. Furthermore, the contribute to variety of cardiovascular diseases (i.e. myocardial infarction). Neutrophils use a large armory kill pathogens including reactive oxygen species (ROS) and Netosis (Branzk N, et al. 2014). The latter one requires the interaction of neutrophil beta2 integrin with the GPIb alpha/ αIIbβ3 on platelets or p-selectin/PSGL-1 complex, respectively (Jenne et al. 2013; Etulain et al. 2015; Caudrillier et al. 2012; Carestia et al. 2016). Intravascular netosis triggers microthrombi formation to seal sites of inflammation and to prevent dissemination of pathogens. This mechanism contributes to a variety of pathological conditions such as thrombosis (Martinod and Wagner 2014; Gould et al. 2015), ischemia/reperfusion injury (Nakazawa et al. 2017; Sayah et al. 2015; Ge et al. 2017; Huang et al. 2013) and tissue-injuries (Czaikoski et al. 2016).

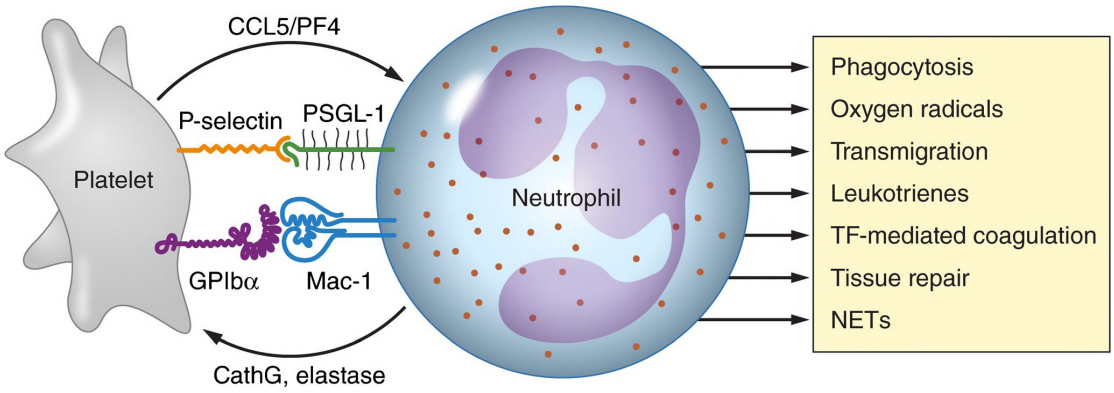

Fig.2.2 Modes of platelet-neutrophil interactions and its consequences (Ton Lisman. 2017).

2.3 Leukocyte-megakaryocyte interaction

In 1956, Humble, et al. described a biological heterozygous “cell-in-cell” phenomenon, termed as “emperipolesis”. Emperipolesis (derived from the Greek words “em” meaning “inside” and “peripolesis” meaning “go around”

Humble et al. 1956) describes the active penetration of one cell by another. The first observation associated with human megakaryocytic emperipolesis was reported by Larsen (Larsen, et al.1970). In comparison to normal cellular engulfment phenomenons, the engulfed cells in the emperipolesis remain intact and viable. Emperipolesis was described in different physiological and pathological conditions (Cashell and Buss, 1992; Mangi and Mufti, 1992; Schmitt et al. 2002). Furthermore, Overholtzer et al. reported recently a homozygous “cell-in-cell” phenomenon, named as “entosis”, bears many similarities with emperipolesis (Overholtzer, et al. 2007).

Thereby, megakaryocytes engulf neutrophils, monocytes or lymphocytes, etc. Emperipolesis mainly appears in different pathological settings. For example, emperipolesis could be found under conditions of thrombocytopenia (Avci Z, et al. 2002), Hodgkin’s lymphoma (Knight Tristan, et al. 2018), acute and chronic leukemia (Shamoto M. 1981), multiple myeloma, and myelofibrosis (Schmitt et al. 2002; Spangrude et al. 2016), blood loss (Cashell and Buss, 1992) and Rosai-Dorfman disease (Cangelosi JJ, et al. 2011). Rosai-Dorfman disease is a rare disorder accompanying with histiocytes hyperproliferation in the lymph nodes, most often in cervical lymph nodes. The viability in extent of emperipolesis is associated with the activity of Rosai-Dorfman disease (Venkateswaran KIyer, et al. 2009) and hence is considered as a clinical hallmarker for diagnostics (Varun Rastogi, et al. 2014). Furthermore, several in vivo animal studies observed emperipolesis within MKs, e.g. after a sublethal irradiation (Bobik R, Dabrowski Z,1995), Leishmaniasis model (Claudia Momo, et al. 2014). Worth mentioning, emperipolesis could also be found in physiological settings, like the megakaryocytic emperipolesis in the fetal liver (Lee WB, et al. 1999). These evidences indicate that emperipolesis is a normal but rare and conservative physiological phenomenon in all the species.

As the physiological role of the process remains still elusive, many groups investigated the underlying molecular mechanism that drives emperipolesis. The study by Overholtzer showed that the formation of the adherence junction is the prerequisite of this entosis process (Overholtzer, et al. 2007). Furthermore, this process requires a Rho-ROCK signaling pathway mediated and myosin-based contractile force change from the recipient cell to allow the penetration of the invading cell (Kroemer G, Perfettini JL. 2014). In this setting integrins are known to regulate cell plasticity and the internalization of the invading cell (Peng Xia, et al. 2008). Previous studies have demonstrated that cancer cells expressing epithelial cadherins (E- or P-cadherins) are able to remodel the epithelial junctions and to engulf non-transfected parental cells in an in vitro growth assay (Overholtzer, et al. 2007). This goes along with the activation of the Rho-ROCK signaling that mediates cytoskeletal rearrangements, within the invading cell.

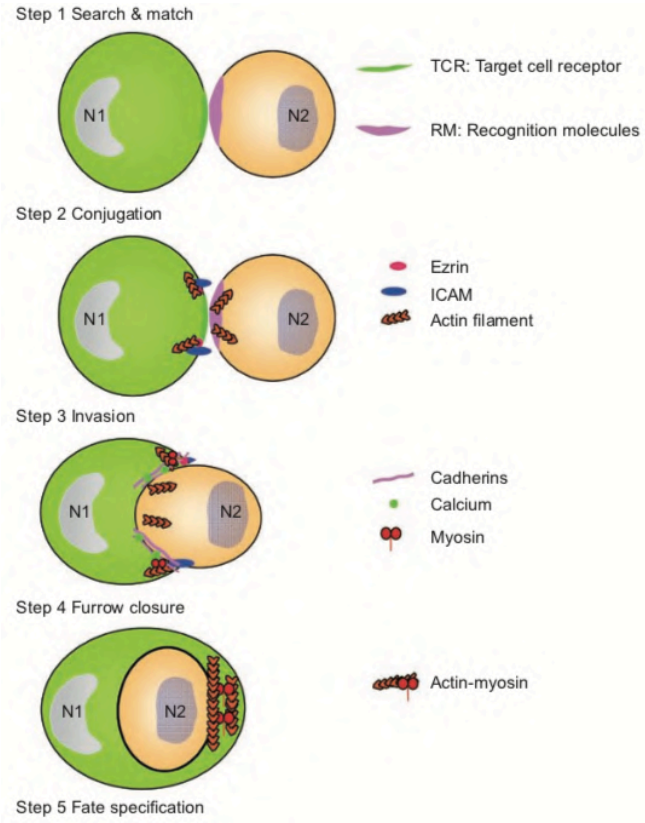

Fig.2.3 Entosis working model (Peng Xia, et al. 2008)

Schmitt et al. reported that TPO-overexpressing megakaryocytes induce myelofibrosis within a mouse model. Furthermore, it increases the incidence of emperipolesis in the bone marrow (Fig.4). Further investigations revealed that this overexpression leads to an augmented fraction of α-granules and further overexpresses P-selectin on the cell membrane of the megakaryocytes, thereby triggering an intensive cytoskeleton remodeling of megakaryocytes (Schmitt A, et al., 2000).

Although distinct molecular mechanisms that drive megakaryocyte emperipolesis have been revealed by different groups, there are still many unanswered questions that needs to be clarified, for instance its physiological and pathological significances. In comparison to normal phagocytosis that will trigger the elimination of the invading by the host cells, emperipolesis will preserve cellular integrity and function and resembles a temporarily event only. Hence, it could be speculated that this phenomenon may be a protecting mechanism for the invading cells to protect them from an otherwise unfavorable microenvironment.

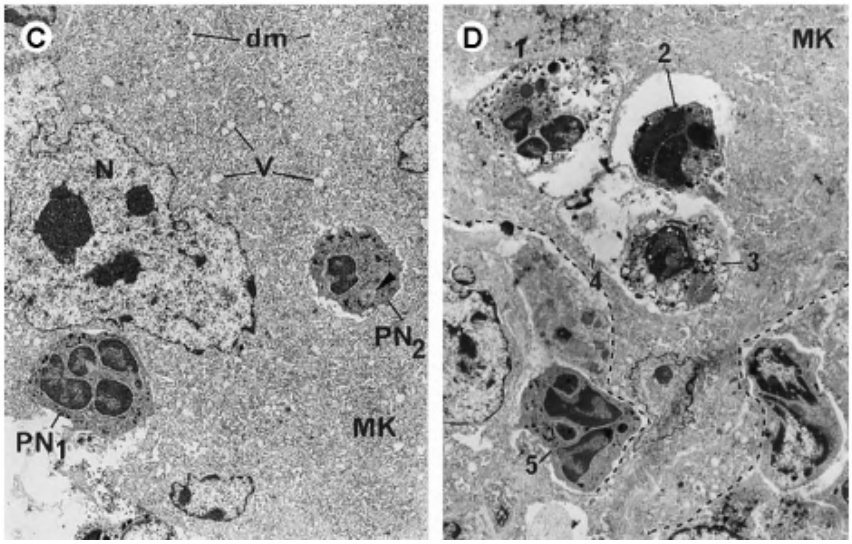

Fig.2.4 Electron-microscopic view of a polymorphonuclear (PMN) cell in the demarcation membrane system (Schmitt A, et al., 2000).

2.4 Thrombopoiesis and platelet production

It is widely accepted that TPO predominantly regulates MK proliferation and differentiation (Choi et al, 1995; Ito et al, 1996, Solar GP, et al. 1998). However, TPO is not involved in later stages of proplatelet forming and shedding. Moreover, the exact molecular mechanisms that regulate proplatelet generation, shedding and platelet biogenesis are still insufficiently understood.

During thrombopoiesis, MKs form cellular extensions, called proplatelets, that protrude those into the blood flow through the vascular sinusoids. Each MK generates thousands of platelets (Kaushansky K.2008). Therefore, MKs have to produce enormous amounts of proteins that allow cellular structure changes or cytoskeleton rearrangements. (Zhang L. et al., 2014, Satoshi Nishimura, et.al, 2015, Kellie R. Machlus, et.l. 2016). Indeed, the most abundant structural protein expressed within MKs is beta1-tubulin. Its genetic deficiency in mice leads to a 60% decrease of platelets counts. Platelets isolated from β1-tubulin null mice exhibit different functional and structural

defects. Along this line, patients with a mutation of β1-tubulin develop an autosomal dominant inherited macrothrombocytopenia (Freson, K., et al. 2005).

In analogy, the highly expressed F-actin regulates proplatelet formation by generating a bifurcation within the proplatelet (Italiano et al., 1999; Patel et al., 2005). In addition to these structural proteins, contractile elements actively contribute to proplatelet formation, especially MYH9 (i.e myosin). In patients that carry mutations within the MYH9 gene macrothrombocytopenia occurs, due to a reduced myosin activity (Althaus K & Greinacher A. 2009). MYH9 deficiency attenuates the initial proplatelet formation within the bone marrow due to a defective Rho-Rho kinase-myosin IIA signaling pathway that results in reduced circulating platelet counts (Chang et al., 2007; Chen et al., 2007). In this context, RUNX1, a transcription factor, has been found to regulate the MYH9 gene expression which may explain the familial platelet disorders in the acute myelogenous leukemia patients, some of whom exhibit a germline heterozygous RUNX1 gene mutation (Bluteau D, et al. (2012).

Nowadays, the progress of live imaging by multiphoton microscopy facilitates the visualization of proplatelet formation in vivo. Junt et al. were first to visualize platelet production in vivo (Junt T. et al., 2007). Afterwards, Zhang et al. have demonstrated that sphingosine 1-phosphate (S1P) signaling through its receptor S1pr1 facilitates the guidance of proplatelets into the blood, likely through the regulation of Src family kinases in MKs (Zhang L. et al., 2014). Recently, a group showed that a different and atypically formed platelet generation is higher under an acute platelet need or inflammatory condition. Their data show that MKs can undergo a rupture like disintegration step to rapidly release huge numbers of platelets to cover the platelet demands under inflammatory conditions. As a possible underlying mechanism, they identified neutrophil derived IL-1α in blood. Whether this process of proplatelet and

platelet biogenesis requires the activation of intracellular caspases is still controversial. Nonetheless, a recent study found that IL-1α signaling through its designated receptor activate caspase-3 that leads to a reduction of membrane stability triggering a final rupture event (Satoshi Nishimura, et.al, 2015).

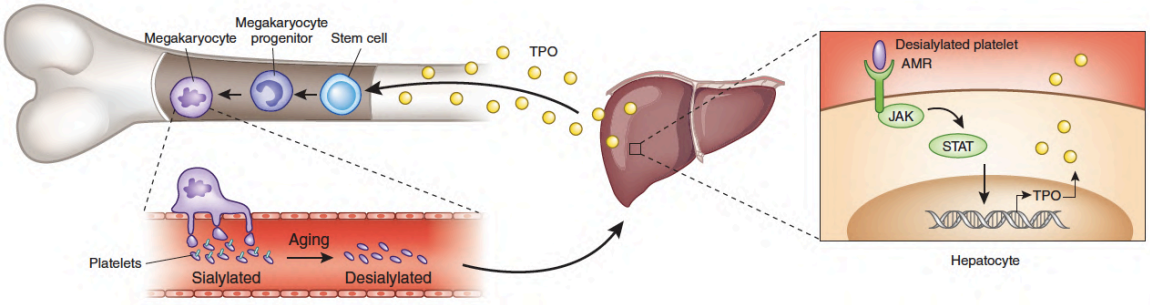

Fig.2.5 Regulation of TPO production (Benjamin T Kile, 2015).

2.5 Conclusion

During thrombopoiesis, proplatelet generation and release occur in a tightly regulated spatial-temporal manner. Within the bone marrow megakaryocytes reside within a very complex niche, in close proximity to various kinds of hematopoietic and immune cells, particularly with neutrophils. However, up to now only little is known about the functional relevance of a direct or indirect MKs-leucocytes interaction and its role on thrombopoiesis. Hence, this project attempts to investigate the leukocytic effects on thrombopoiesis and provides us a new concept about whether and how immune cells are involved in the mechanism of the proplatelet forming and shedding in vivo.

3. Materials and methods

3.1 Mice strains

C57BL/6 mice were purchased from Charles River company. Pf4-Cre mice (Tiedt, Schomber et al. 2007), Rosa26-Confetti mice (Livet J; et al. 2007), Lysm-eGFP mice (Faust N, et al. 2000), CD41-eYFP mice (Zhang J, et al. 2007) were purchased from the Jackson laboratory. Rosa26idtr_Mrp8^{Cre} mice, Mrp8^{Cre}_CXCR4$^{flox/flox}$transgenic mice, and Mrp8^{Cre}_CXCR4f$^{lox/flox}$_Lysm-eGFP mice were kindly provided by Prof. Andrés. Hidalgo. P22phox mutated mice were kindly provided by Prof. Görlach. To generate Rosa26-Confetti_Pf4Cre_Lysm-eGFP triple knock in mice, we first crossed the Rosa26-Confetti mouse with Pf4Cre mouse line before being crossed with Lysm-eGFP mouse line. All animal experiments were approved by the Bavarian government and met the demands of Bavarian legislation concerning animal protection.

3.2 Materials

3.2.1 Antibodies

Name	Clone	Company	Catalog number
Ultra-LEAF Purified anti-mouse Ly-6G Antibody	1A8	Biolegend	127649
Ultra-LEAF Purified Rat IgG2a, κ Isotype Ctrl Antibody	RTK2758	Biolegend	400544
Ultra-LEFA Purified Rat	R86-8C5	Biolegend	108453

anti-mouse Ly6G/Ly6C (Gr-1)			
Ultra-LEAF™ Purified anti-mouse CD11a Antibody	M17/4	Biolegend	101118
FITC Hamster Anti-Mouse CD61	HMβ3-1	BD Pharmingen	553346
FITC Rat Anti-Mouse CD3 Molecular Complex	17A2	BD Pharmingen	555274
FITC anti-mouse CD41 Antibody	MWReg30	Biolegend	133904
FITC Rat IgG1, κ Isotype Ctrl Antibody	RTK2071	Biolegend	400405
FITC Hamster IgG1 κ Isotype Control A19-3	A19-3	BD Pharmingen	553971
PE anti-mouse CD115 (CSF-1R) Antibody	AFS98	Biolegend	135506
PE Rat Anti-Mouse Ly-6G	1A8	BD Pharmingen	551461
PE anti-mouse CD41 Antibody	MWReg30	Biolegend	133906
PE Rat IgG1, κ Isotype Ctrl Antibody	RTK2071	Biolegend	400408
APC anti-mouse Ly-6G/Ly-6C (Gr-1) Antibody	R86-8C5	Biolegend	108412
APC anti-mouse/rat CD42d Antibody	1C2	Biolegend	148506
CD45R (B220) Monoclonal Antibody, PE-Cyanine5	RA3-6B2	eBioscience	15-0452-82
CD144 (VE-cadherin) Monoclonal Antibody, Biotin	16B1	eBioscience	13-1449-82
GFP Polyclonal Antibody		Invitrogen	A-11122
GP IXb-Alexa 488	Kindly provide by Prof. Nieswandt		

3.2.2 Reagents

Name	Company	Catalog number
Thiazole Orange	Sigma-Aldrich	390062
Recombinant Mouse Thrombopoietin	Immunotools	12343615
Neutrophil Isolation Kit, mouse	Miltenyi Biotec	130-097-658
Monocyte Isolation Kit (BM), mouse	Miltenyi Biotec	130-100-629
Pan T Cell Isolation Kit II, mouse	Miltenyi Biotec	130-095-130
LD Columns	Miltenyi Biotec	130-042-901
Dulbecco's Modified Eagle's Medium	Sigma-Aldrich	D8537
L-15 Medium (Leibovitz)	Sigma-Aldrich	L1518
EZ-Link™ Sulfo-NHS-Biotin	Thermo Scientific	21217
Apocynin	Sigma-Aldrich	A10809
Qtracker 705 Vascular Labels	Invitrogen	Q21061MP

3.2.3 Machines and software

Name	Company	Version
Centrifuge	Eppendorf	5804R
Two photon microscope	LaVision Biotec	TriM Scope II Series
Confocal microscopy	Zeiss	LSM 900
Hematology analyzer	IDEXX	ProCyte Dx
Flow cytometer	Beckman Coulter	Gallios

Cryotome	Lecia	CryoStar NX70
Prism Graphpad	Prism	7
IMARIS software	IMARIS	7.2.1 and 8.2.1
Flowjo software	Treestar	8.7

3.3 Methods

3.3.1 Neutrophil depletion in mice

For neutrophil depletion in Rosa26^{idtr}/Mrp8^{Cre} mice, diphtheria toxin (DT), which was prediluted with PBS to achieve a final dose of 10ng/g bodyweight, was intraperitoneally (i.p) injected. Each mouse received a consecutive 5-days treatment with DT.

For antibody mediated neutrophil depletion, 10-12 weeks-old C57BL/6 mice, Confetti-PF4Cre/Lysm-eGFP or CD41eYFP mice received intravenously (i.v) 50µg Ly6G purified antibody (clone RB6-8C5) or isotype control every second day for three times.

3.3.2 Multiphoton intravital live imaging

The preparation of the calvaria bone was described before (Zhang L. et al., 2014). First, 10-12 weeks-old mice received an anesthesia with 5.0 Vol. % Isoflurane and 2% oxygen, followed by an i.p. injection of MMF solution (90µl Midazolam (0.5mg/kg), 90µl Fentanyl (5mg/kg) and 15µl Meditomidin (0.05mg/kg)) with a repetitive injection every 45 min. Next, hair on the head was removed by a shaver and hair removal solution (MAXIM, Köln Germany). Afterwards a PE-10 polyethylene catheter was placed into the murine tail vein using tissue glue for the fluid administration. After incision of mouse partial skin

on the front calvarium and exposure of midline and frontoparietal skull, a custom metal ring was immobilized on the skullcap with metal glue which allowed the application of PBS or ultrasound gel respectively to prevent tissues drying during imaging. The mouse head was immobilized with custom metal holder and the mouse was placed on a heating pad to maintain body temperature. A LaVison Biotech intravital multiphoton scope system based on Ti:sa laser and OPO laser, equipped with a 16X water immersion objective, NA 0.95 (Nikon, Germany) was used to visualize the mouse calvarium and to capture images. In Confetti_Pf4Cre_Lysm-eGFP mouse model, eGFP fluorescence and confetti fluorescence (particular RFP) were detected by Ti:sa laser with an 800nm wavelength and OPO laser with a 1050nm wavelength. In CD41YFP-Ly6G-PE mouse model, YFP fluorescence and PE-labeled neutrophils were detected by a compromised 910nm wavelength. The vasculature was visualized by administration of 15µl Qtracker705; which was detected in 800nm with a near infrared channel (US695/H). For 4 dimensional image acquisition, image stacks were captured at an aforementioned wavelength with a 1-2µm imaging depth per layer over a total depth of 20-50µm with a plan region of interest of 405×405µm every 60 seconds over 1hour. To generate and analyze 4D movies, original data were reconstructed by IMARIS software (version 7.2.1 and 8.2.1). Following parameter will be determined: number of MK-leukocyte interactions, interaction times, proplatelet length, releasing time and speed. To analyze the sphericity of MKs, the surface of MKs was constructed by IMARIS software based on the fluorescence of MKs. The sphericity of MKs can be automatically analyzed by the IMARIS software.

3.3.3 Fetal liver derived and bone marrow derived MKs culture

Fetal liver cell derived megakaryocytes were generated from fetal livers (E13.5-14.5) which were subsequently cultured in Dulbecco's Modified Eagle Medium (DMEM; Invitrogen, Germany) with supplementary of 10% Fetal bovine serum, 1% penicillin and streptomycin and 70ng/ml mouse Thrombopoietin (mTPO) for 4-5 days to acquire mature megakaryocytes in the humidified 5% CO2 incubator at 37℃ as previously described (Jonathan N. Thon, et al. 2010). Subsequently mature MKs were purified and enriched using a bovine serum albumin (BSA) gradient (from top to bottom, PBS-1.5%BSA-3%BSA) before being harvested after 30 minutes from the sediment.

Similarly, in order to acquire the bone marrow derived megakaryocytes, adult mouse bones were harvested and bone marrow was flushed with 2% FBS/PBS. Bone marrow suspension was cultured for 4-5days in Dulbecco's Modified Eagle Medium (DMEM; Invitrogen, Germany) with a supplementary of 10% Fetal bovine serum, 1% penicillin/streptomycin and 70ng/ml mouse Thrombopoietin (mTPO) as well as 15UI/ml heparin. At day 4 cells were collected with the same BSA gradient method as aforementioned.

3.3.4 Measurement of reticulated platelets

Murine whole blood was collected by cardiac puncture using an ACD buffer treated tube. 20µl whole blood was fixed with 1% PFA at room temperature for 10 minutes and thereafter washed with PBS in a 15ml falcon. Platelets then were stained in 100µl PBS with 1µg/ml thiazole orange and 1µl CD42d-APC. Afterwards the population of reticulated platelets was gated and determined by thiazole orange and CD42d-APC double positive.

3.3.5 Platelet lifespan measurement

Mice were intravenously injected with Sulfo-NHS-Biotin (30mg/kg) (Thermofishcer, Gemany) through the lateral tail vein. Beginning at day one after biotinylation, 20µl blood was collected from the tail vein in ACD (Acid citrate dextrose) buffer, diluted into 100µl PBS buffer and stained with 1µl CD42d-APC antibody and 1µl streptavidin-PE antibody at 4℃ in a dark place for 30 minutes. The fraction of biotinylated streptavidin bound platelets was detected after gating for CD42d positive platelets. At day one 100% of platelet were streptavidin positive, though the percentage of this cell population decreased over time, Platelet lifespan was determined by linear regression analysis.

3.3.6 Neutrophils adoptive transfer

Mouse bones were collected from donor C57BL/6 mice or genetic knock out mice. For PMN homing experiments, neutrophils were harvested from Lysm-eGFP mice or $Mrp8^{CXCR4}$/Lysm-eGFP mouse which express enhanced green fluorescent proteins in PMN.

For isolation bones were cut at the end and bones marrow was flushed with 2%FBS/PBS. After collection of the bone marrow, neutrophils were isolated according to the manuals of mouse neutrophils isolation kit (Miltenyi biotec, Germany). Afterwards, 2.500.000 neutrophils were injected via lateral tail vein into recipient mouse. One hour after the adoptive transfer, the recipient mice were sacrificed and perfused with PBS and 4% PFA. Thereafter mouse femoral, humoral and tibia bones from recipient mice were harvested and then incubated firstly in 15% sucrose and 30% sucrose, sequentially. Finally, bones were frozen in Tissue Tec at -80℃ before being stained using whole mount staining technique.

3.3.7 Whole mount bone staining

Frozen Bones were cut horizontally. Next bones were blocked in a 10% goat serum with 0.1% triton X-100 for 1 hour at room temperature. Thereafter bones were incubated in PBS with primary antibodies overnight to label transferred neutrophils, vessels and megakaryocytes, respectively. After incubation and washing, bones were visualized by confocal microscopy or multiphoton microscopy.

3.3.8 Quantification of platelet associated fragments

Sterile 6 well plates were coated with 100µg/ml fibrinogen at 37℃, for one hour and blocked with 1.5% BSA afterwards. Megakaryocytes and neutrophils were isolated using the BSA gradient method or PMN isolation kit (Miltenyi biotec, Germany) as mentioned above. In order to measure the impact of neutrophils on the release of platelet associated fragments, a different numbers of megakaryocytes (10.000, 25,000 and 50,000) were seeded in the 6 well plates and then co-cultured with 2.500.000 neutrophils in culture-medium (40% DMEM medium+10%FBS+1% penicillin/streptomycin) + 60% L-15 medium) for 6 hours at 37℃. After 6 hours, the supernatant of each well was collected and fixed with 1%PFA for 10 minutes. After washing with PBS, the pellet was stained with 1:100 concentration of CD42d-APC, CD61-FITC and Ly6G-PE antibody mix.

3.3.9 Immunostaining

Coverslips were washed with ethanol and distilled water sequentially before being coated with 100ng/ml fibrinogen. Megakaryocytes and neutrophils were seeded on the coverslips and co-cultured in the mix medium (40% (DMEM medium+10%FBS+1% penicillin/streptomycin) + 60% L-15

medium) at 37℃ for 6 hours. Thereafter cells were fixed with 4% paraformaldehyde for 10 minutes and then washed with PBS. All the cells were permeabilized with 0.1% NP40 for intracellular protein staining. Cells were incubated with different primary antibodies at room temperature for 2 hours or 4℃ overnight and then in secondary and conjugated antibodies for 2 hours at room temperature. Primary antibodies and secondary antibodies included Ly-6G purified antibody (Biolegend, San Diego, USA), CD144 antibody (Biolegend, San Diego, USA), CD41-FITC antibody, Stromal cell-derived factor-1 antibody (Cell signaling technology, Massachusetts, USA)

3.3.10 Blood count measurement

Mouse blood was harvested by cardiac puncture, collected in an ACD buffer tube (the ratio between ACD and blood is 1:7) and analyzed by a hematology system (IDEXX ProCyte DX).

Human blood samples from healthy donors were drained by venous puncture using a specified single-use citrate pretreated container (Sarstedt) and measured in an automatic hematocytometer system in Klinikum der LMU München.

3.3.11 Flow cytometry and cell sorting

Cells was surface stained in FACS buffer (PBS supplemented with 2% FBS) on ice for 30 minutes. Multiparameter flow cytometric analysis was performed using a Gallios Flow Cytometer (Beckman Coulter). Neutrophils were gated by Ly6G. T cells and B cells were gated by CD3 and CD45R, respectively. Monocyte population was identified by GR-1^{high}, $CD115^{high}$. Following antibodies were used: Ly6G-PE(1A8), CD3-FITC (17A2), CD45R-Pecy5(RA3-6B2), CD115-PE (AFS98), GR-1-APC (RB6-8C5).

3.3.12 LFA-1 antibody blocking experiment

For the LFA-1 blocking experiment, 10-12 weeks-old C57BL/6 mice received 50μg CD11a purified antibody (clone M17/4) or isotype control antibody intravenously (i.v) every second day, three times in total.

3.3.13 Statistics analyses

Data was analyzed using Prism7 (GraphPad) and presented as mean±SEM (standard error of mean). A p-value <0.05 was considered as statistically significant. Student's t test was used for two groups comparison. Statistics analysis of multiple group comparison based on the One-way ANOVA followed by Tukey's multiple comparison test.

4. Results

4.1 The absence of neutrophil in vivo attenuates the platelet production

4.1.1 Diphtheria toxin (DT) induced neutrophil depletion in Rosa26^{iDTR}_Mrp8^{cre} mice results in reduced platelet counts

In order to investigate the role of leukocytes, in particular of neutrophils, in thrombopoiesis in vivo, we first used Rosa26^{iDTR}/Mrp8^{cre} mice, which express diphtheria toxin receptor under control of a neutrophil specific Mrp8 promotor, to see how platelet counts change within the peripheral blood under an acute neutropenic condition.

A consecutive 5 day treatment with diphtheria toxin (DT) (0.01µg/g bodyweight) almost entirely abolished peripheral neutrophils within the bloodstream (**Fig.4.1.1.2**). Meanwhile, white blood cell counts showed a 35% decrease and platelet counts also presented a 30% decline in mice, showing a thrombocytopenic phenotype (**Fig.4.1.1.2**). The thrombocytopenic phenotype indicated either the platelet production or clearance altered after induction of neutropenia. Hence, the reticulated platelets (young platelets) were assessed with flow cytometry technique by gating the thiazole orange and CD42d-APC double positive population in all blood cells. The reticulated platelet fractions showed a reduction in the absence of neutrophils (**Fig.4.1.1.3**), indicating the platelet biogenesis was to some extent blunted. In the meantime, the platelet lifespan in the course of treatment were also similar in both groups (**Fig.4.1.1.4**). The percentage of biotinylated platelets had no significant variation in both groups every day, suggested the ablation of neutrophils would

not affect the cell -involved (i.e. Macrophages) platelet clearance. The number of mature MK is also of importance to determine the platelet production in the mouse. The flow cytometric assessment of MK progenitors or mature MKs in the bone marrow did not show relevant difference in both groups as well (**Fig.4.1.1.5**). Worth mentioning, a previous study has demonstrated that mature MKs with high content of DNA are susceptible to produce platelets. Hence, MKs ploidy measurement is also useful and necessary to examine MK maturation after 5 days DT treatment. Based on our flow cytometry analysis (**Fig.4.1.1.6**), MK ploidy likewise did not show relevant difference in these two groups. The data of above-mentioned two assessments indicated neutrophil depletion would not affect the megakaryopoiesis. Taken together, we concluded that the absence of neutrophils in mice impacts on thrombopoiesis rather than on megakaryopoiesis.

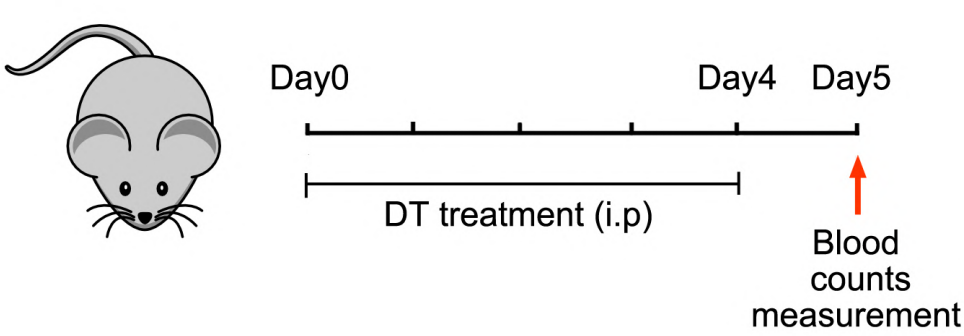

Fig.4.1.1.1 Treatment scheme of DT induced neutropenia

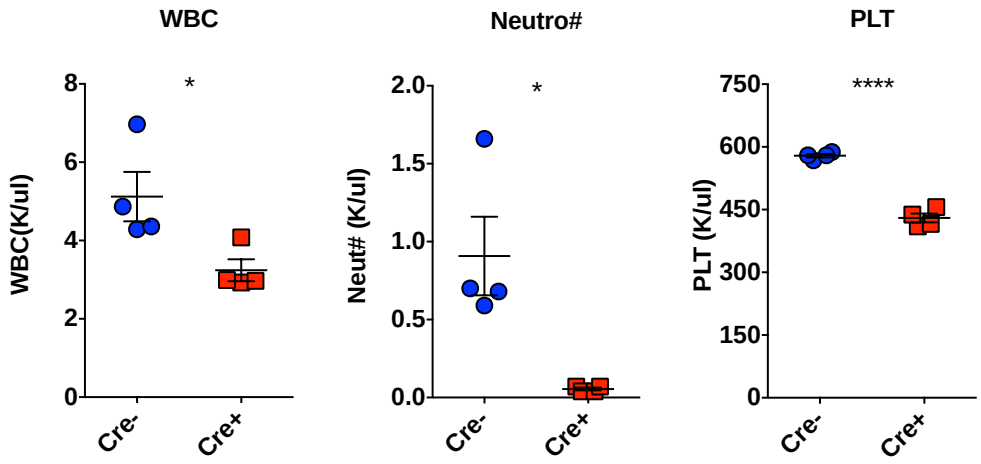

Fig.4.1.1.2 Diphtheria toxin (DT) treatment results in a marked reduction of platelet counts in Mrp8-Cre positive mice

blood analyzed at day5, N=4 per group, error bars, mean±SEM *P<0.05, **P<0.01, ****P<0.0001, data represent two independent experiments analyzed with unpaired Student's t-test.

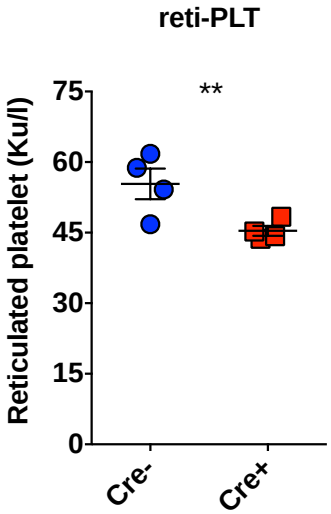

Fig.4.1.1.3 Circulating reticulated platelet fragments (young platelets) assessed by flow cytometry with thiazole orange staining

N=4 per group, error bars, mean±SEM *P<0.05, **P<0.01, data represent two independent experiments analyzed with unpaired Student's t-test).

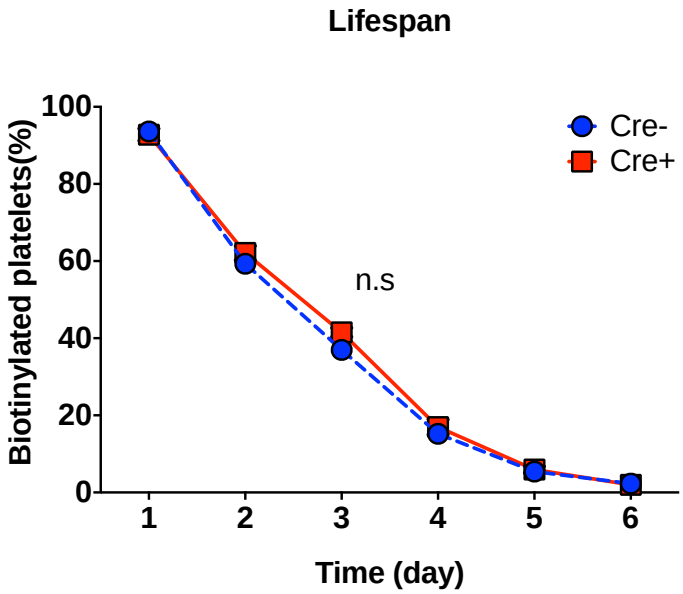

Fig.4.1.1.4 Assessment of platelet lifespan in $Mrp8^{Cre+}$ and $Mrp8^{Cre-}$ littermate control mice over time with DT treatment

blood samples were collected from tail vein at the same time point of each day, N=4 per group, error bars, mean±SEM, n.s, (non-significant), data analyzed with paired Student's t-test).

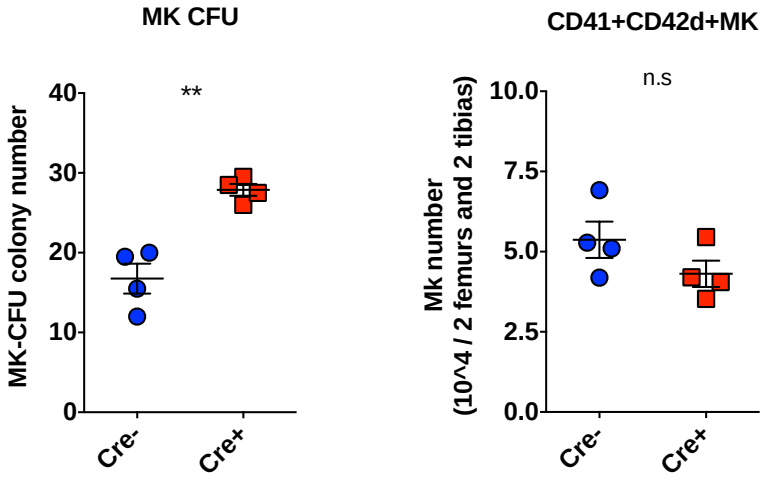

Fig.4.1.1.5 Quantification of megakaryocytic progenitors and mature MK numbers in Mrp8^{Cre+} mice and their littermate controls after DT treatment

N=4 per group. error bars, mean±SEM *P<0.05, **P<0.01, n.s. (non-significant), data representing two independent experiments analyzed with unpaired Student's t-test.

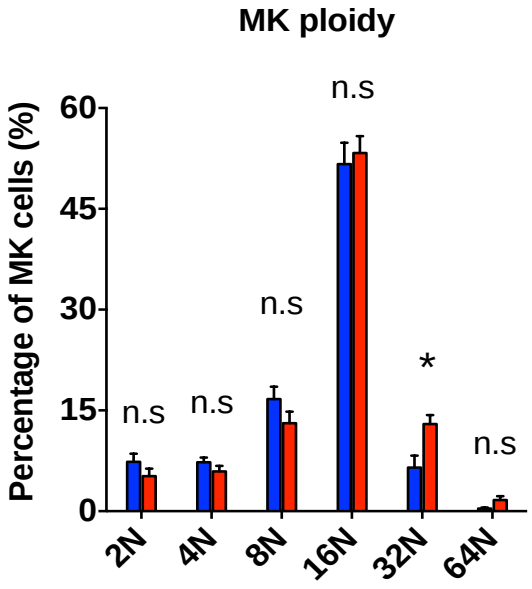

Fig.4.1.1.6 MK ploidy assessed by flow cytometry after DT treatment

N=4, error bars, mean±SEM, n.s non-significant, data representing two

independent experiments analyzed with one-way ANOVA test.

4.1.2 Antibody mediated neutrophil depletion leads to a thrombocytopenic phenotype

To verify that the collected data was not mouse-specific, we performed a widely used neutropenic mouse model by Ly6G/Ly6C (clone RB6-8C5) antibody mediated neutrophil depletion in C57BL/6 mice. The same treatment scheme of DT induced neutropenia was adopted (**Fig.4.1.2.1**). Within this model, the application of Ly6G/Ly6C antibody induced the reduction of WBC and neutrophil counts in peripheral blood (**Fig.4.1.2.2**). Interestingly, platelet counts displayed a continuous decline about 23% on day 3 and 30% on day 5 in comparison to their littermate controls (**Fig.4.1.2.2**). And this data indicated that the reduction of platelet counts under neutropenic condition was indeed time- and neutrophil-dependent. Thereafter we assessed the reticulated platelet fractions on day 0, day 3 and day 5, respectively (**Fig.4.1.2.3**). The platelet counts did not show a drastic drop followed by continuing neutrophil depletion on day 5, but reticulated platelet production still remained low yield on day 5. In analogy, platelet lifespan assays demonstrated that neutrophils do not alter platelet clearance in the time course of antibody induced neutropenia (**Fig.4.1.2.4**). Mature MK counts and MK maturation (i.e. ploidy) were not affected by this neutrophil depletion antibody as well according to our flow cytometry analyses (**Fig. 4.1.2.5 and Fig. 4.1.2.6**). Moreover, maximal MK diameter and MK counts in the humeral bones were assessed by using multiphoton microscopy imaging techniques, and no phenotypic changes of MKs were found in both two groups, indicating no alteration of megakaryopoiesis within this neutropenic model. In combination with the data from $Rosa^{iDTR}$_$Mrp8^{cre}$, the absence of neutrophils indeed leads to a reduction

of platelet counts in the mouse through attenuating the platelet biogenesis in vivo.

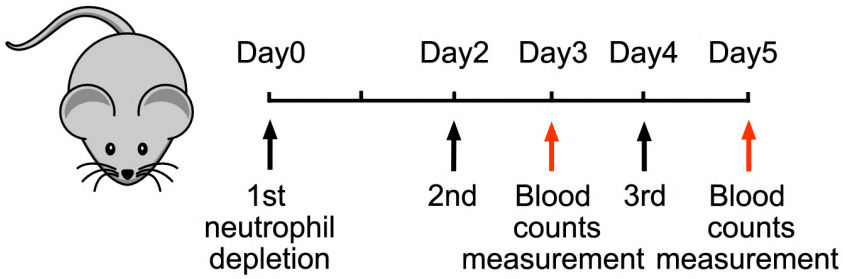

Fig.4.1.2.1 Ly6G/Ly6C antibody treatment scheme in C57BL/6 mice

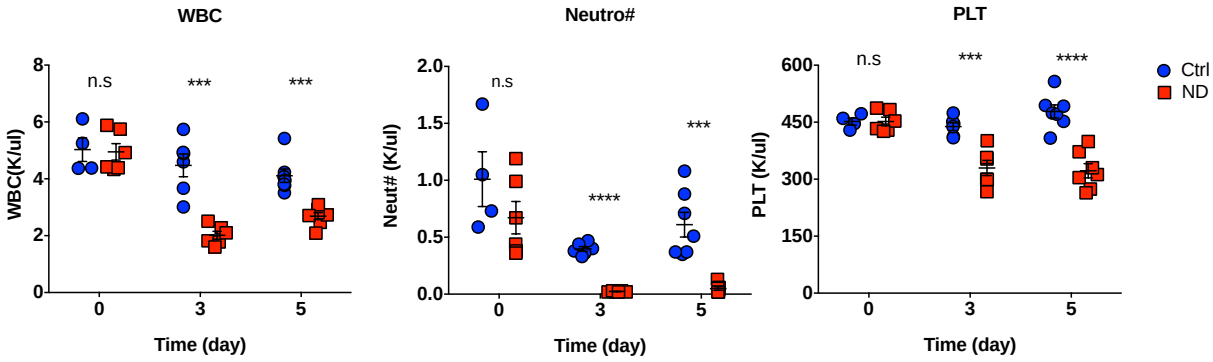

Fig.4.1.2.2 Antibody mediated neutrophil depletion leads to reduced platelet counts in C57BL/6 mice

N=4-7 per group, error bars, mean±SEM, ***P<0.001, ****P<0.0001 n.s non-significant, data represents 3 independent experiments analyzed with unpaired Student's t-test.

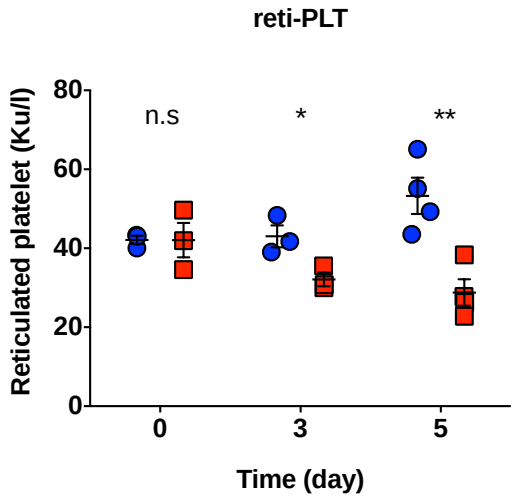

Fig.4.1.2.3 Reticulated platelet production is attenuated after neutrophil depletion

N=3-5 per group, error bars, mean±SEM *P<0.05, **P<0.01, n.s non-significant, data representing 2 independent experiments analyzed with unpaired Student's t-test.

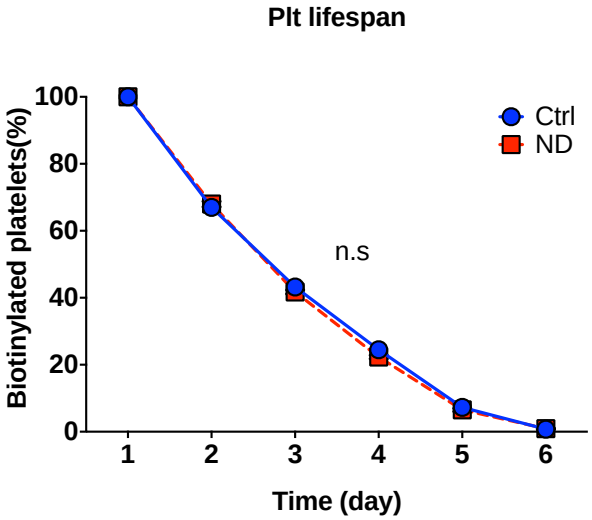

Fig.4.1.2.4 Platelet lifespan did not change during the time course of treatment by Ly6G/Ly6C depletion antibody

N=4 per group, error bars, mean±SEM, n.s non-significant, data analyzed with

paired Student's t-test.

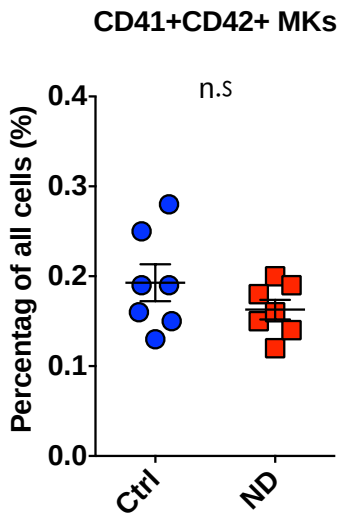

Fig.4.1.2.5 Quantification of mature MK numbers by FACS in C57BL/6 mice

N=7, error bars, mean±SEM, n.s not significant, data representing 3 independent experiments analyzed with unpaired Student's t-test.

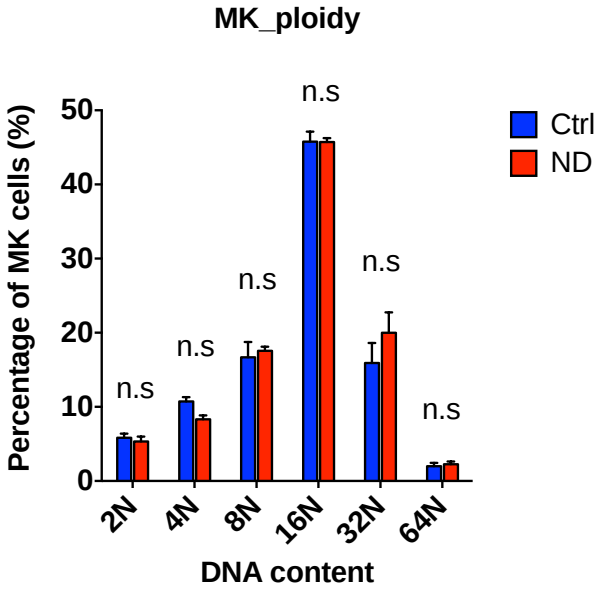

Fig.4.1.2.6 Flow cytometric quantification of MK ploidy in C57BL/6 mice

On day 5, MK ploidy was assessed by quantification of propidium iodide intensity. N=4, error bars, mean±SEM *P<0.05, **P<0.01, n.s non-significant, One way ANOVA test was used to determine the statistical significance.

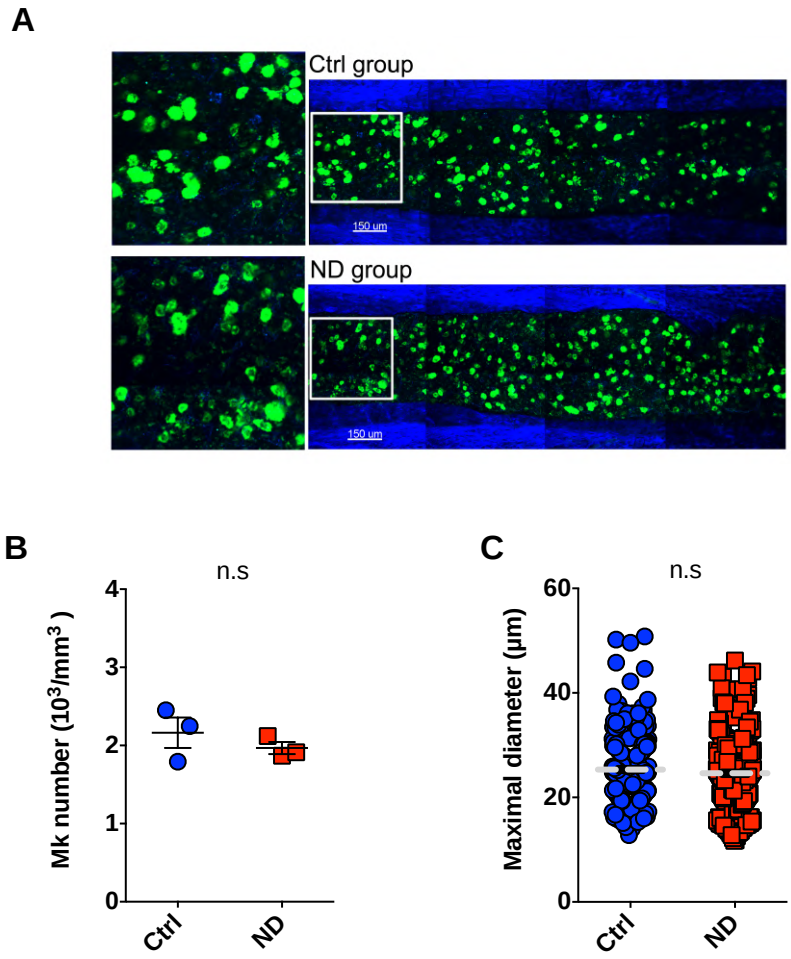

Fig.4.1.2.7 MK characterizations after antibody induced neutropenia in C57BL/6 mice

(A) representative whole-mount picture of humeral bones (B) MK number quantification (C) and maximal diameter of MKs were analyzed by IMARIS software (N=3, error bars, mean±SEM *P<0.05, **P<0.01, n.s non-significant, data analyzed with unpaired Student's t-test).

Next we wanted to investigate the leukocyte subsets specificity of our findings. Therefore we took advantage of a catchup mouse line. The catchup mouse is a kind of genetic mouse in which Ly6G locus is modified with a knock-in allele encoding Cre recombinase and the tdTomato fluorescent protein. Neutrophils show no Ly6G expression in homozygous mice and 50% more expression in the heterozygous ones.

To exclude side- and off-target effects of Ly6G/Ly6C antibody (RB6-8C5 clone) in mice, the same neutrophil depletion strategy was adopted in catchup mice (**Fig.4.1.3.2**). As figure **4.1.3.3**) shows, WBC and neutrophil counts decreased in the bloodstream of heterozygous mice as usual and platelet counts also showed a decline. In contrast WBC and neutrophil counts remain stable after Ly6G/Ly6C antibody treatment in homozygous mice due to the deficiency of Ly6G on neutrophils. Importantly, platelet counts did not change over time. This data once again demonstrated PMN was the reason that resulted in reduced platelet yields in the mouse.

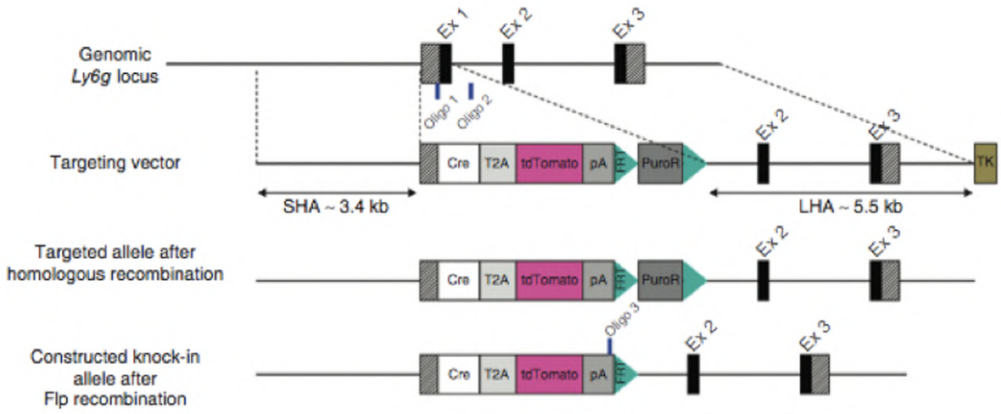

Fig.4.1.2.8 Representative of targeting strategy for the generation of catchup mice (data from Anja Hasenberg，Nature Methods，2014)

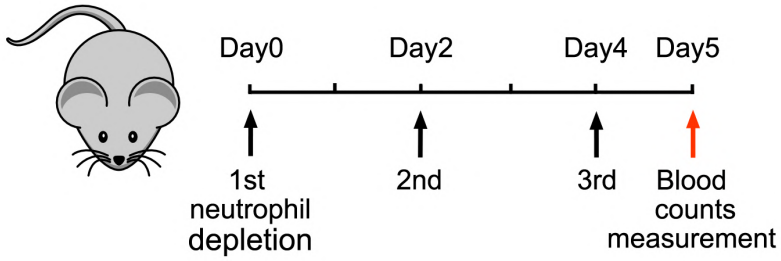

Fig.4.1.2.9 Ly6G/Ly6C antibody treatment scheme in catchup mice

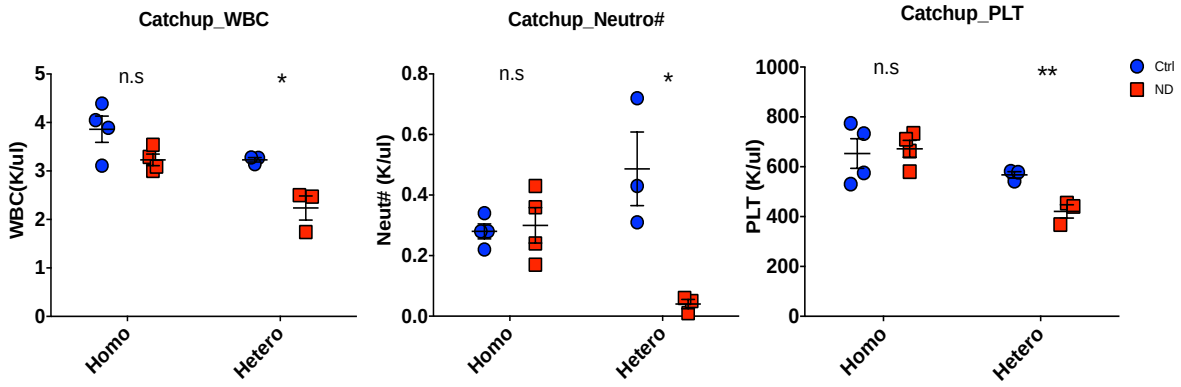

Fig.4.1.2.10 Antibody mediated neutrophil depletion leads to reduced platelet counts in catchup heterozygous mice, but not in homozygous ones (N=3-4, error bars, mean±SEM *P<0.05, **P<0.01, data analyzed with unpaired Student's t-test).

`

4.2 Role of MK-PMN interactions in vitro

4.2.1 Augment PAF release from MKs in vitro

Based on our data from both murine acute neutropenia models, we demonstrated that neutrophils play a prominent role during the final steps of platelet biogenesis in vivo. Given the intrinsic limitation and complexity of MK-PMN interaction in vivo, we established an in vitro co-culture model (**Fig.4.2.1.1** and **Fig.4.2.1.2**) to examine and investigate the effects of molecules or cell types on thrombopoiesis.

Sphingosine 1-phosphate (S1P) has been identified as an agonist that can amplify the MKs' proplatelet fragmentation in vivo and in vitro (Zhang L. et al., 2014). Hence we verified this results by treating MKs with 10μM S1P, after 6 hours co-culturing, bone marrow derived MKs (**Fig.4.2.1.3**) yielded increased PAF numbers when stimulated by S1P alone and importantly when co-cultured with PMNs. We further tested the impact of different ratios between MK and neutrophil numbers. Indeed, we found that PAF number decreased with lower ratios of MK/PMN.

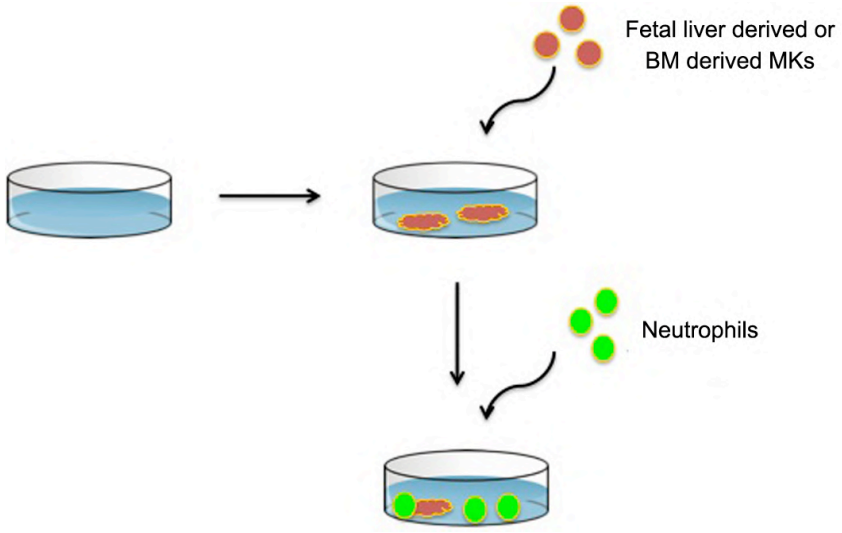

Fig.4.2.1.1 Schematic overview of in vitro co-culture procedure.

Cells were co-incubated for 6 hours; supernatants were collected and PAF

numbers quantified by flow cytometry.

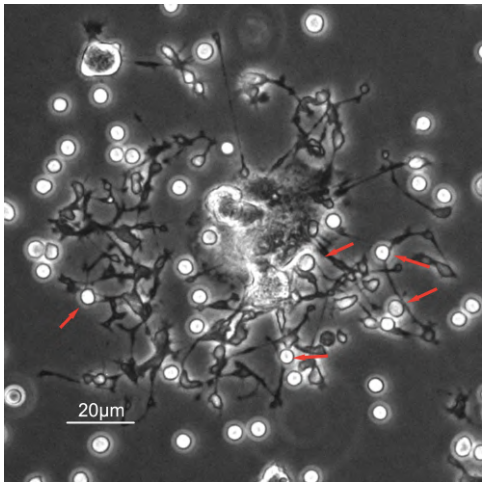

Fig.4.2.1.2 Bright field microscopy image of a bone marrow derived MK interactions with PMNs in vitro

red arrows indicate the MK-PMN interactions, scale bar, 20 μm

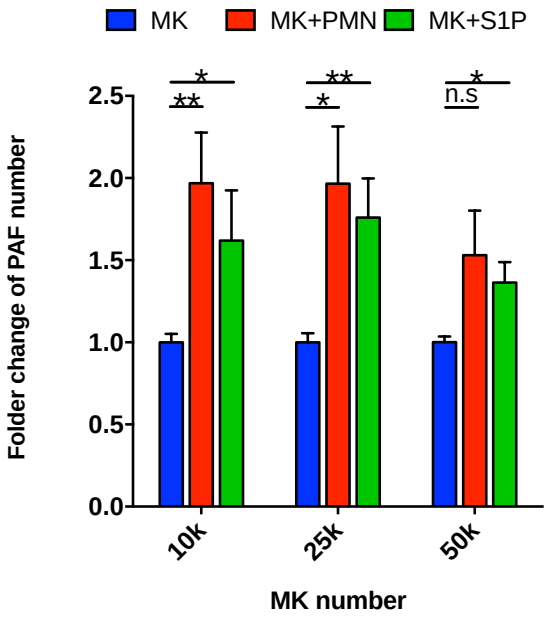

Fig.4.2.1.3 Quantification of platelet associated fragment (PAF) numbers

after MK-PMN co-culture

PAF counts of indicated co-culture MK(k, thousand) - PMN(250,000) groups were normalized before comparison with vehicle group(blue), N=4, error bars, mean±SEM *P<0.05, **P<0.01, n.s non-significant, data representing 4 independent experiments, One-way ANOVA followed by Tukey's multiple comparison test was used to determine the statistical significance.

4.2.2 Impact of different white blood cell (WBC) populations on PAF generation

Given that different population of white blood cells are found in the peripheral blood as well as within the bone marrow, it was essential to examine the effects of other WBCs on thrombopoiesis (i.e. lymphocytes). We adopted our in vitro co-culture model to examine the effects of other cell types on PAF production. Hence we examined the effect on the role of T-cells and monocytes by seeding either pan-T cells or monocytes (250,000 cells) on top of the MKs. Of note the number of monocytes and lymphocytes within the BM is lower than PMN numbers hence the in vitro ratio between either cell type and MKs may by overestimated in our model. As shown in **Figure.4.2.1.4**, monocytes augmented PAF numbers in the supernatant, while T-cells have no effect on PAF formation. The effect of monocytes was robust for all three tested MK numbers.

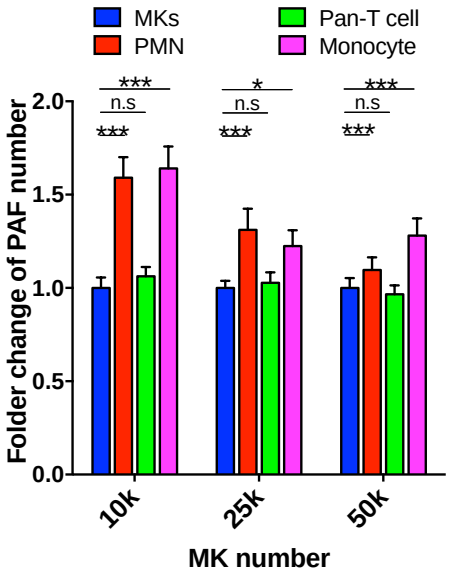

(data share by Christian Weber)

Fig.4.2.1.4 Flow cytometric quantification of PAF counts in the supernatant after co-culture with indicated WBC subsets

N=3-4, error bars, mean± SEM. *P<0.05, ***P<0.001, n.s non-significant, data representing 4 independent experiments, One-way ANOVA followed by Tukey's multiple comparison test was used to determine the significance.

4.2.3 A physical interaction between PMNs and megakaryocytes is required to promote PAF release in vitro

Cell-to-cell communications occurs through direct physical interaction or paracrine mechanisms mediated by cytokines or chemokines respectively. To address which mechanism contributes to PAF formation in our setting we performed trans-well assays. Hence, a Boyden chamber assay was established to examine whether neutrophils accelerated proplatelet forming through direct physical interactions. An insert with a pore size of 0.4μm was placed on top of cultured MKs at the bottom of the dish, to prohibit PMN-MK

interactions (**Fig.4.2.3.1**). As done before the same number of neutrophils was seeded in the upper chamber. Our data suggest that released cytokines or chemokines do not increase PAF number in vitro but rather require a direct physical interaction.

To further elaborate on this question MKs were cultured in supernatant of phorbol myristate acetate (PMA) stimulated PMNs. However supernatants also did not show a PAF-augmenting capacity, underscoring that neutrophils derived cytokines or chemokines are not necessary for the PAF release in our in vitro assay.

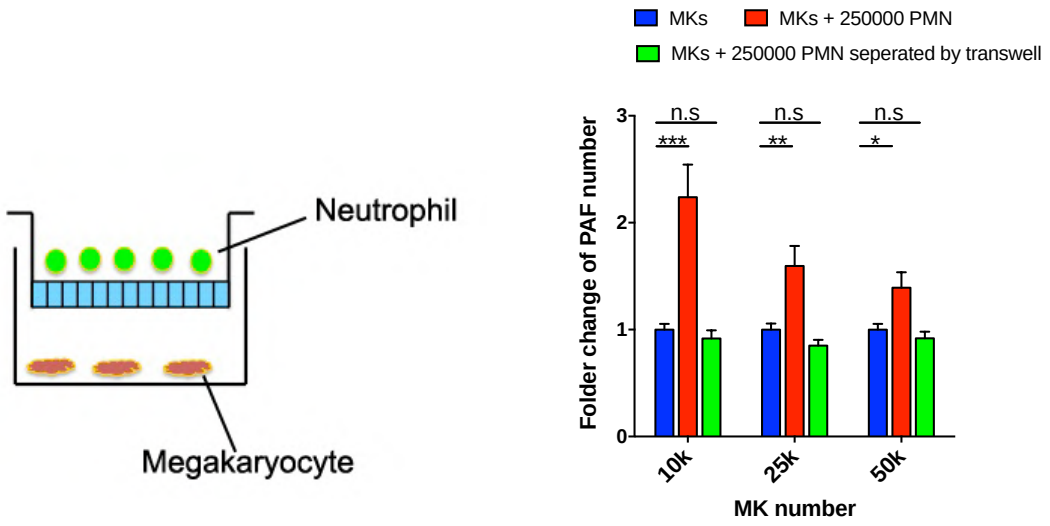

(data shared by Christian Weber)

Fig.4.2.3.1 Flow cytometric analysis of PAF counts in a modified tran-swell model

A trans-well chamber with a pore size 0.4µm containing neutrophils on the top and MKs were seeded in the bottom of six wells. N=3, error bars, mean±SEM *P<0.05, **P<0.01, ***P<0.001, n.s non-significant, data representing 3 independent experiments, One-way ANOVA followed by Tukey's multiple comparison test was used to determine the significance.

4.2.4 Inhibition of PMN mobility reduced the effects of PMNs on PAF release

We found that neutrophil mediated platelet fragmentation in vitro needs a direct physical interaction with MKs. Hence, the inhibition of PMN migration or other motile actions should decrease PAF release in vitro. Therefore, we repeated our co-culture experiment following PMN treated with cytoskeleton protein inhibitors, like cytochalasin D, Blebbistatin and nocodazole. The fungi toxin Cytochalsin D specifically inhibits actin polymerization by depolymerizingd the actin filament organization. Blebbistatin is widely used to selectively inhibit the activity of myosin II ATPase and to blunt the cell motility functions. Nocodazole is an agent, that exerts effects in cells by interfering with the microtubule polymerization and is commonly used in oncology.

Neutrophils were pre-incubated with 100nM Cytochalsin D, 50nM Blebbistatin and 50nM Nocodazole, respectively, for 30 minutes before being co-cultured with MKs. As shown in **Fig.4.2.4.1**, neutrophils treated with Cytochalasin D and Blebbistatin lost their function of PAF augmentation in vitro with comparison to sham and Nocodazole, which may be due to the defect of physical interaction with MKs. This data also suggested that actin-myosin driven neutrophil motility is required to drive PAF production.

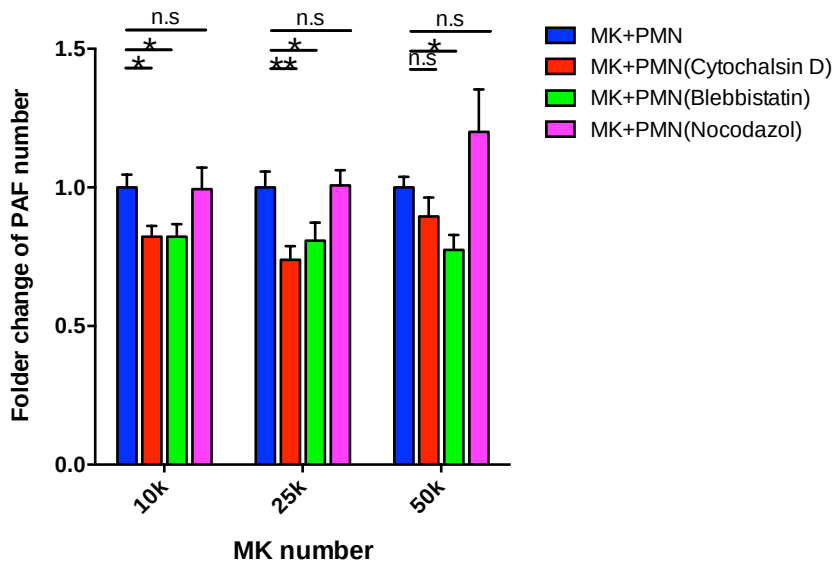

Fig.4.2.4.1 Flow cytometric quantification of PAF number in vitro model co-culture with cytoskeletal protein inhibitors treated PMNs

N=3, error bars, mean±SEM *P<0.05, **P<0.01, n.s non-sifnificant, data representing 3 independent experiments, One-way ANOVA followed by Tukey's multiple comparison test was used to determine the significance.

4.3 Proplatelet fragmentation in vivo is attenuated in the absence of PMNs

4.3.1 PMN-MK interactions occur more frequently with highly proliferative MKs

Previous data has demonstrated positive effects of neutrophils on platelet biogenesis in vivo and vitro. So far we do not know how effect thrombopoiesis in vivo. Therefore, we established a calvarium imaging model to visualize physical MK-PMN interactions in vivo to characterize interaction dynamics.

For the calvarium model (**Fig.4.3.1.1**) 5µg Ly6G-PE was injected (i.v) into

the CD41eYFP mouse 30 minutes before the imaging. CD41eYFP reporter gene mice express enhanced yellow fluorescence in megakaryocytes. In our preliminary test, Ly6G-PE antibody was able to label neutrophils in peripheral blood and the bone marrow approximately one hour after injection (**Fig.4.3.1.2**). Hence, using multiphoton intravital microscopy (MP-IVM) the neutrophils (red) and megakaryocytes (yellow) could be clearly distinguished and visualized within the calvarial bones and bloodstream (**Fig.4.3.1.3**).

By using this model, we visualized the physical interactions between neutrophils and MKs with different maturity and tried to characterize their interaction patterns. In order to better characterize MKs a mathematic parameter, Waddell sphericity index ($\psi = \frac{\sqrt[3]{\pi(6\mathrm{VP})^2}}{\mathrm{AP}}$), was introduced to describe the angularity of the observed objects. The Waddell sphericity index ranges from 0 to 1. The sphericity value of MKs displays an inverse relationship of cell angularity, meaning that more angulated proplatelet-forming MKs have a lower sphericity (**Fig.4.3.1.4A**). In CD41eYFP mouse, MKs showed a gaussian distribution of their sphericity (**Fig.3.3.1.5A**). However, we found that PMN interact with all different categories of the MKs (**Fig.4.3.1.4B**). Moreover, the ratio analyses of proplatelet-forming MK (PPF MK) to none proplatelet-forming MK (None-PPF MK) suggested that low sphericity MKs had a stronger capacity to form proplatelets (**Fig.4.3.1.5B**).

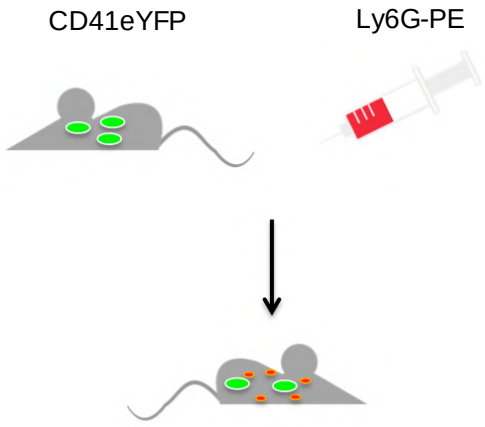

Fig.4.3.1.1 The schematic overview of CD41eYFP/Ly6G-PE antibody dual reporter model

CD41eYFP mouse received one dose (5 μ g) of PE labeled Ly6G (clone 1A8) to visualize neutrophils during the in vivo imaging.

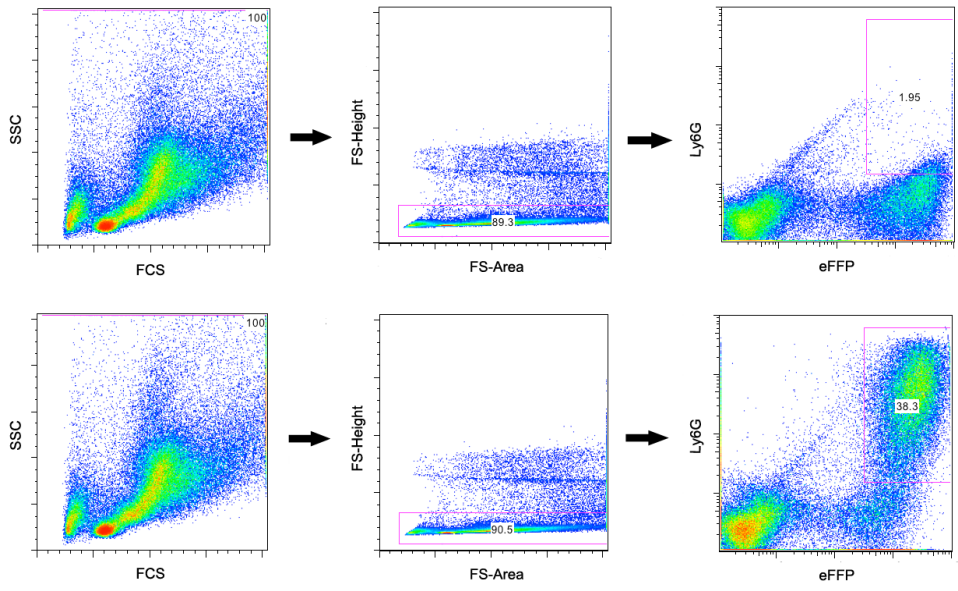

Fig.4.3.1.2 Gating strategy of bone marrow PMNs in Lysm-eGFP mouse 1 hour after Ly6G-PE i.v injection

PMNs in bone marrow were sorted by eGFP^{Posi} and Ly6G-PE^{Posi} population,

this population can be sorted in bone marrow indicates Ly6G-PE is able to penetrate into the BM and label BM neutrophils during in vivo imaging.

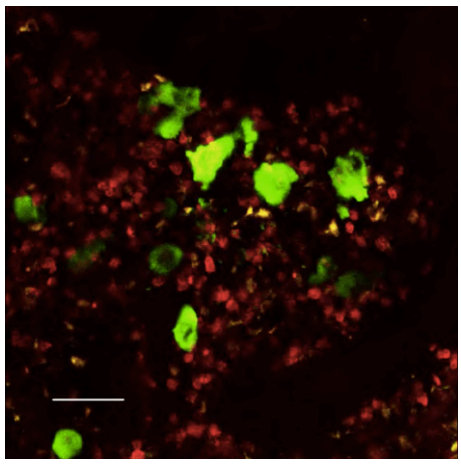

Fig.4.3.1.3 Representative image of MK-PMN interactions in carvarial compartment of CD41eYFP/Ly6G-PE mouse

MKs and PMNs show green and red fluorescence, respectively. scale bar, 50μm

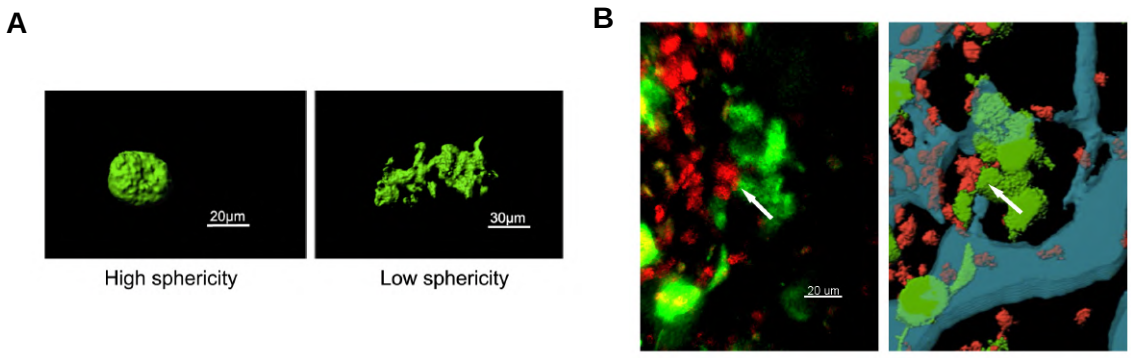

Fig. 4.3.1.4 3D reconstruction of MK-PMN interactions in vivo by IMARIS software.

(A) representative 3D reconstructed picture of MKs with different Waddell sphericity indices and (B) a representative image, reconstructed from a video of CD41eYFP/Ly6G-PE dual reporter mouse (6 layers, 18μm depth) (MKs, PMNs and vessels are shown in green, red and cyan colors, respectively. scale bar, as indicated in the images.

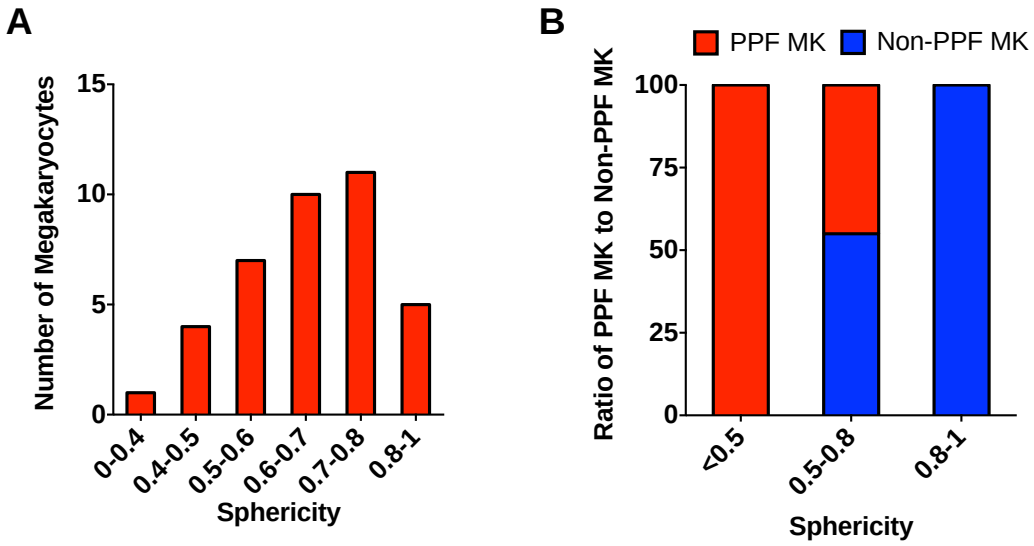

Fig.4.3.1.5 Sphericity indices can be used to discriminate MK proliferation in vivo

(A) MKs display a gaussian distribution (B) Highly proliferative, proplatelet forming MKs have lower sphericity indices (<0.5), low proliferative, round MKs have indices between 0.8-1. (8 videos and 40 MKs were analyzed)

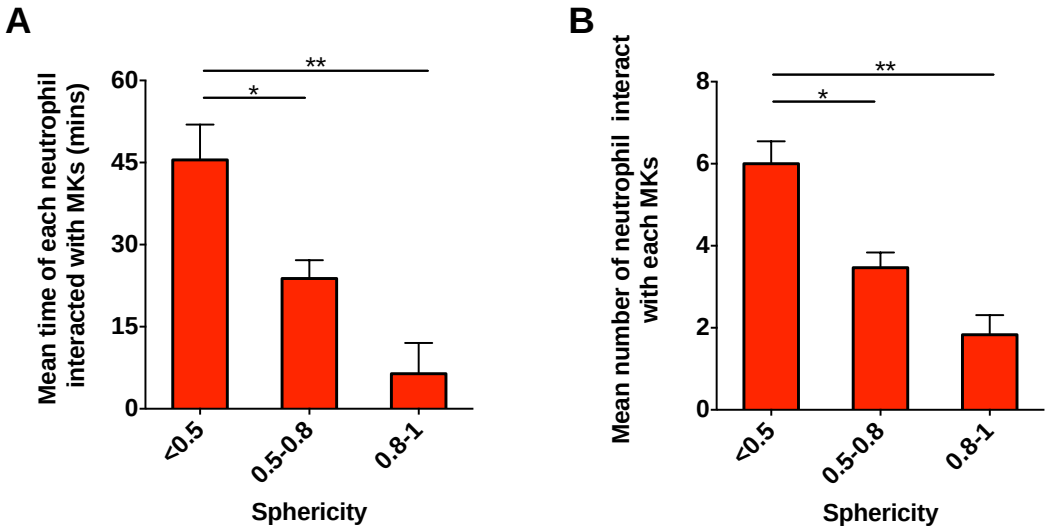

Fig.4.3.1.6 Quantification of MK-PMN interaction time and interacted PMN numbers in CD41eYFP/Ly6G-PE model

(A) mean time of each PMN and (B) mean number of PMNs interacted with each MK during the in vivo imaging (8 videos and 40 MKs were analyzed, error bars, mean±SEM *P<0.05, **P<0.01, data represents 8 independent experiments analyzed with One-way ANOVA followed by Tukey's multiple comparison test).

4.3.2 Proplatelet formation dynamics in vivo

Our data demonstrated that antibody mediated neutrophil depletion can lead to reduced platelet counts through blunting the platelet biogenesis in mice. To further elaborate on this, we visualized proplatelet formation during the thrombopoiesis in the presence or absence of neutrophils. As usual, we firstly demonstrated that antibody-mediated neutrophil depletion yields reduced platelet counts in CD41eYFP mice (**Fig.4.3.2.1**). Thereafter we visualized proplatelet forming and shedding of CD41eYFP mouse in the absence or

presence of neutrophils. In the control group, proplatelet growth was constant without any retractions. In contrast, under neutropenic condition, proplatelet growth was slower and the release was delayed, did repetitive retraction of the proplatelet.

In detail (**Fig.4.3.2.2**), the number of proplatelets released by MKs per hour was less in the absence of neutrophils; due to an increased proplatelet releasing time. However, the maximal length of proplatelet, displayed no statistically significant difference between the two groups, indicating that the absence of neutrophil would not impact on the MK proplatelet forming, rather on proplatelet releasing and shedding speeds. In a second approach we used another reporter mouse model (Confetti Pf4/Lysm-eGFP mouse) to visualize the PMN-MK interactions during thrombopoiesis (**Fig.4.3.2.3**). Again under neutropenic conditions proplatelet releasing times were prolonged and the amount of released proplatelets was reduced. However, as seen before the maximal length of proplatelets showed no significant difference in both groups. Interestingly, MK-PMNs interaction decreased within the vasculature niche but not within the bone marrow niche. This is in line with our observation from our Rosa^{iDTR}_Mrp8^{cre} mouse model which showed that an additional abolishment of neutrophils inside the BM niche does not lead to an increase in platelet reduction beyond the observed 30%, seen within the antibody depletion model. Taken together, this finding suggested a dominant role of PMN-MK within the vascular nice on thrombopoiesis.

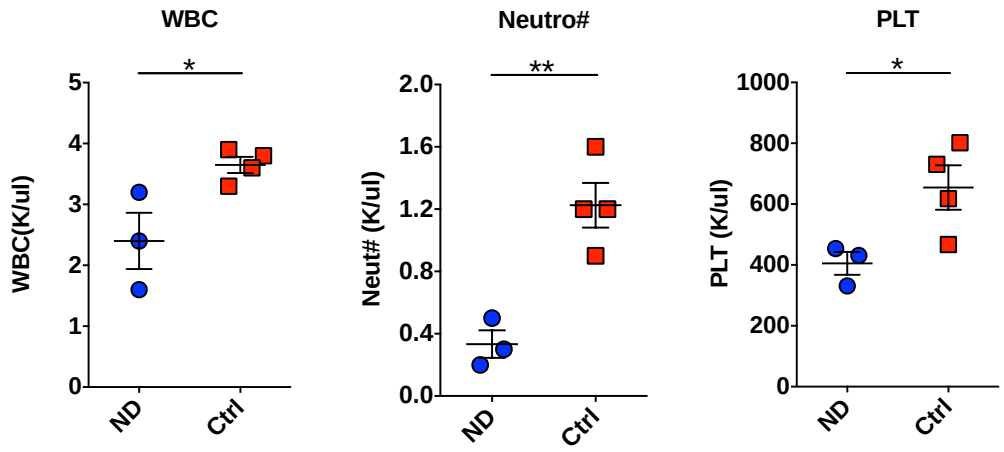

Fig.4.3.2.1 Peripheral blood counts in CD41eYFP mice after 3 times antibody mediated neutrophil depletion

N=3-4, error bars, mean±SEM *P<0.05, **P<0.01, data represents 2 independent experiments and were analyzed with unpaired Student's t-test.

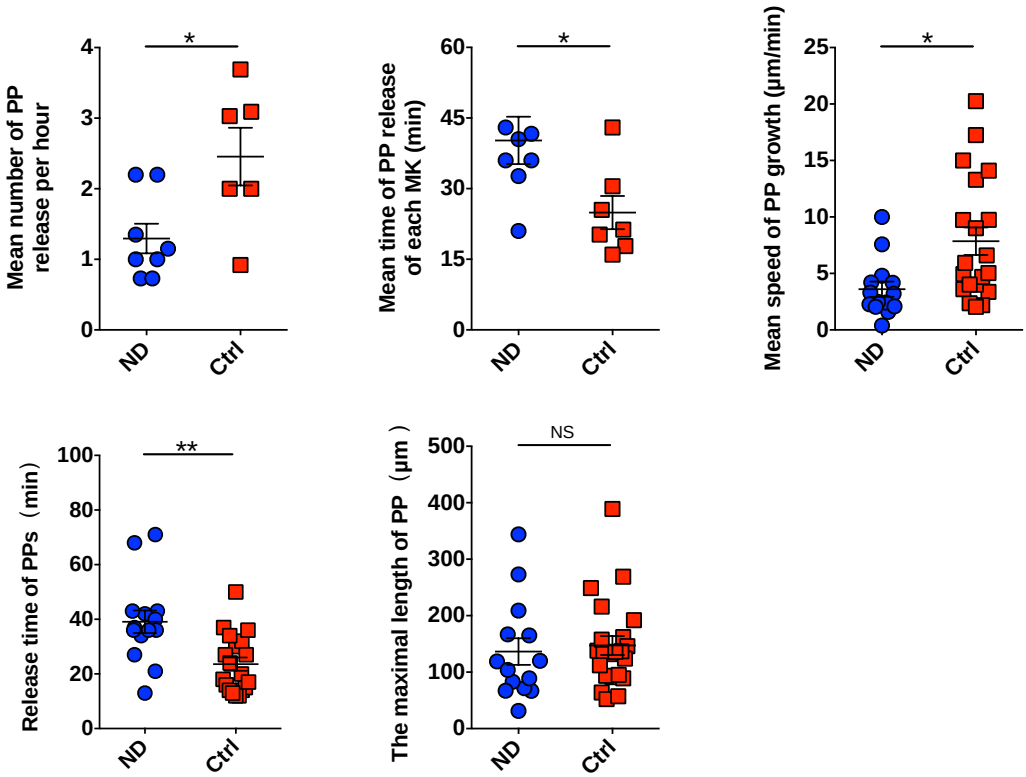

Fig.4.3.2.2 Quantification of MK proplatelet formation in CD41eYFP/Ly6G-PE antibody dual reporter model under steady and neutropenic conditions.

N=3-4, error bars, mean±SEM *P<0.05, **P<0.01, NS, not significant, data represents 7 independent experiments analyzed by IMARIS software and statistical significance was determined with unpaired Student's t-test.

4.4 Spatial resolution of PMN-MK interactions during thrombopoiesis

4.4.1 PMNs within the vascular niche drive proplatelet fragmentation

To assess the role of PMNs in circulation pool, in a second approach we used another reporter mouse model (Confetti Pf4/Lysm-eGFP mouse) to visualize the PMN-MK interactions during thrombopoiesis (**Fig.4.4.1A**). In confetti Pf4/Lysm-eGFP mouse, cell intrinsically express red fluorescence in MKs and green fluorescence in PMN cells under the control of Pf4 promotor and Lyz2 promotor, respectively. Again under neutropenic conditions proplatelet releasing times were prolonged and the amount of released proplatelets was reduced. However, as seen before the maximal length of proplatelets showed no significant difference in both groups. Interestingly, MK-PMNs interaction decreased within the vasculature niche but not within the bone marrow niche (**Fig.4.4.1B**). This is in line with our observation from our $Rosa^{iDTR}$_$Mrp8^{cre}$ mouse model which showed that an additional abolishment of neutrophils inside the BM niche does not lead to an increase in platelet reduction beyond the observed 30%, seen within the antibody depletion model.

Taken together, this finding suggested a dominant role of PMN-MK within the vascular nice on thrombopoiesis.

In the absence of neutrophils (neutrophil elimination only in the circulation) over 5 days platelet counts are progressively decreasing in C57BL/6 mice displayed a progressively decreasing trend (reduced by 23% and 30% at day 3 and 5, respectively). Rosa26^{iDTR} x Mrp8^{Cre} mice also exhibited a 30% reduction in platelet counts under neutropenic conditions for constitutive 5 days. However, neutrophil elimination in both BM and vasculature pools in Rosa26^{iDTR} x Mrp8^{Cre} mice did not show additional platelet reduction or deterioration of their thrombocytopenic phenotype in the mouse. Video analysis found that most neutrophils in the circulation locate to the budding sites of proplatelet forming megakaryocytes (**Fig.4.4.2**). These data might indicate that bone marrow resident neutrophils are less important compared to neutrophils within the vascular niche. In particular, adhesive neutrophils surrounding the budding sites of proplatelet forming MKs (dash circles area in **Fig.4.4.2)** seemed to play the dominant role during the thrombopoiesis.

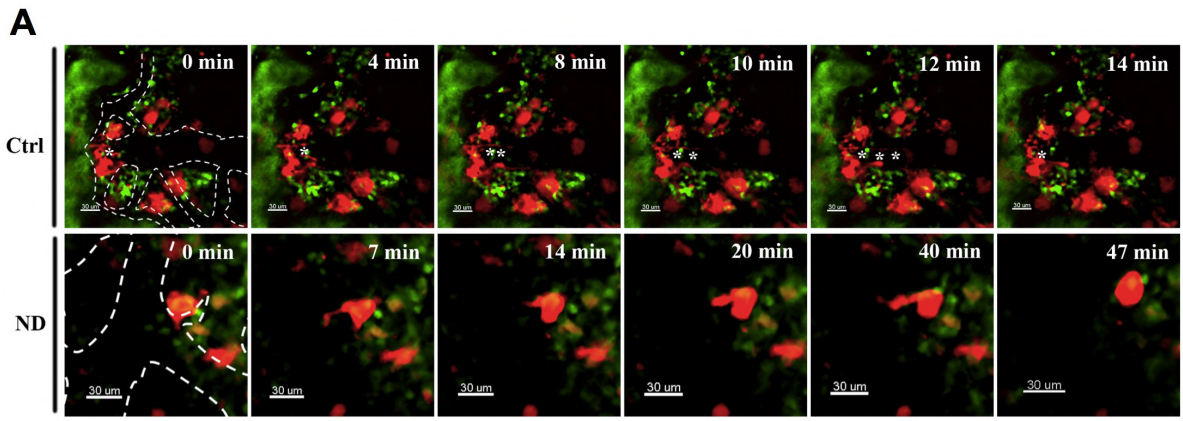

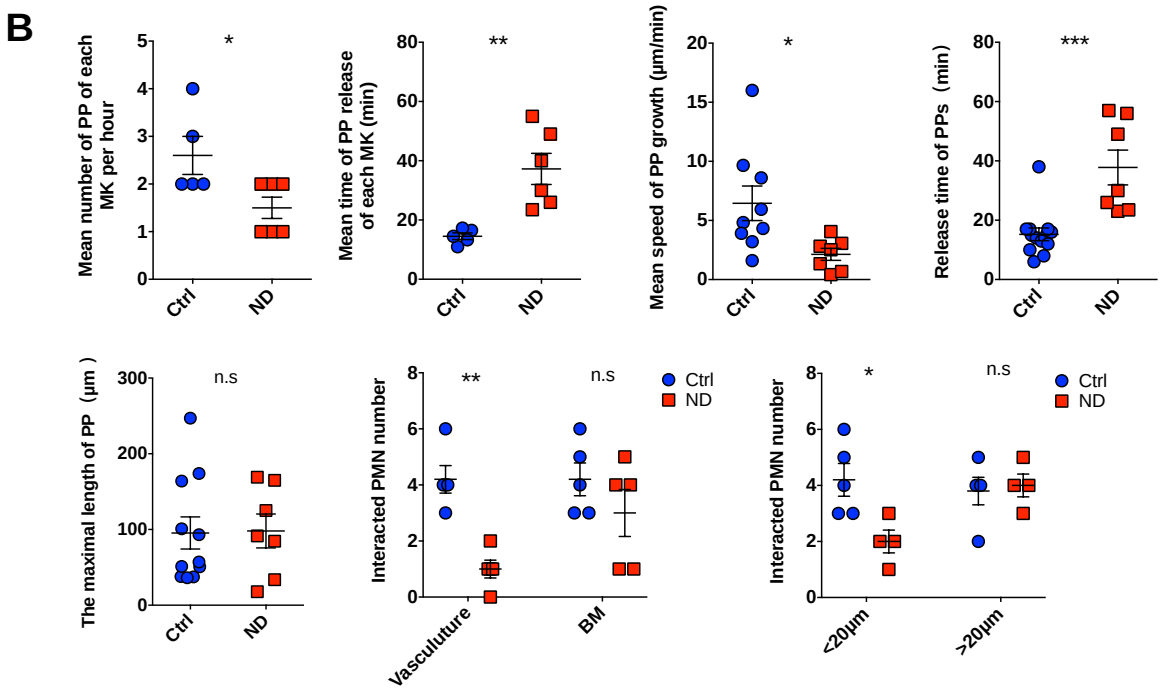

Fig.4.4.1 Quantification of proplatelet formation in Confetti PF4/Lysm-eGFP dual reporter model under steady and neutropenic conditions.

(A) representative images of proplatelet forming process under steady or neutropenic condition; (B) Analysis of proplatelet releasing numbers, time, growth speed, and interacted PMN numbers in circulation and bone marrow niches. (N=3 per group, error bars, mean±SEM *P<0.05, **P<0.01, n.s not significant, MKs and PMNs show red and green colors, respectively. Dash line indicates the vessel. scale bar, 30μm, data representing 6 independent experiments analyzed with unpaired Student's t-test).

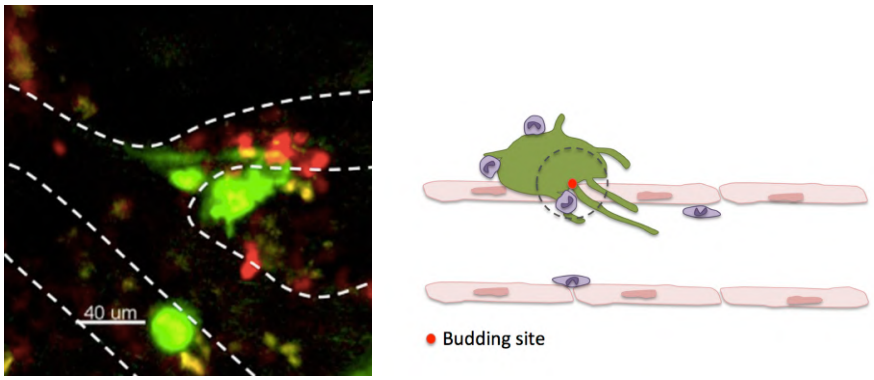

Fig.4.4.2 Representative images of neutrophils gathering around the budding site of PPF-MKs

MKs and PMNs show the green and red fluorescence, respectively. Dash line indicates the vessel, scale bar, as indicated in the picture.

4.4.2 MK-PMN interactions during thrombopoiesis are ICAM-1 dependent

Above introduced data demonstrated the PMN-MK interactions in the vasculature niche play a pivotal role during the thrombopoiesis, especially those in proximity to the budding sites of proplatelet forming MKs (Fig.3.4.1) This observation is further underscored by flow cytometry analyses of the different neutrophil depletion models. To further elucidate the underlying molecular mechanism, we focused on known molecules which have been identified earlier as mediators of interaction between neutrophils, platelets or endothelial cells including P-selectin, integrin beta2, PSGL-1 and ICAM-1, etc. After the blocking these molecules in the circulation compartment, we did not see a significant reduction of platelet counts in vivo (data not shown), except for ICAM-1 blocking (**Fig.4.4.2.1**). ICAM-1 consists of two subunit molecules, CD11a and CD18. ICAM-1 can be specifically blocked by a LFA-1(CD11a) antibody which leads to reduced platelet counts without altering neutrophil

numbers. Meanwhile, flow cytometry analyses indicated that LFA-1 antibody only attenuates reticulated platelets (**Fig.4.4.2.2**) but not mature MK numbers (**Fig.4.4.2.3**) or MK maturation (i.e. ploidy) (**Fig.4.4.2.4**). Furthermore, cell number of other white blood cells did not show big variation within the bloodstream and bone marrow (**Fig.4.4.2.5A and Fig.4.4.2.5B**). Taken together, all data indicate that ICAM-1 impacts on the regulation of the PMN-MK interaction during the thrombopoiesis.

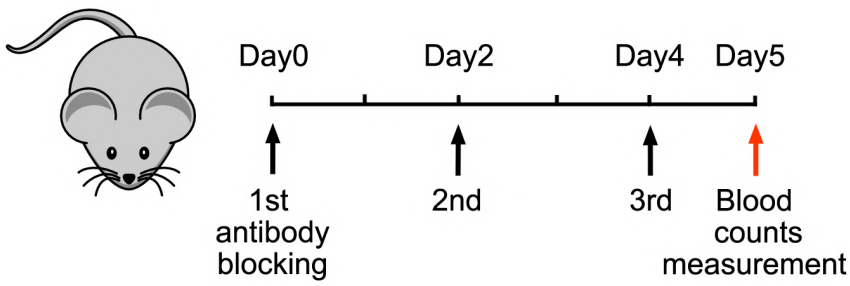

Fig.4.4.2.1 Treatment scheme of LFA-1 antibody blocking in C57BL/6 mouse

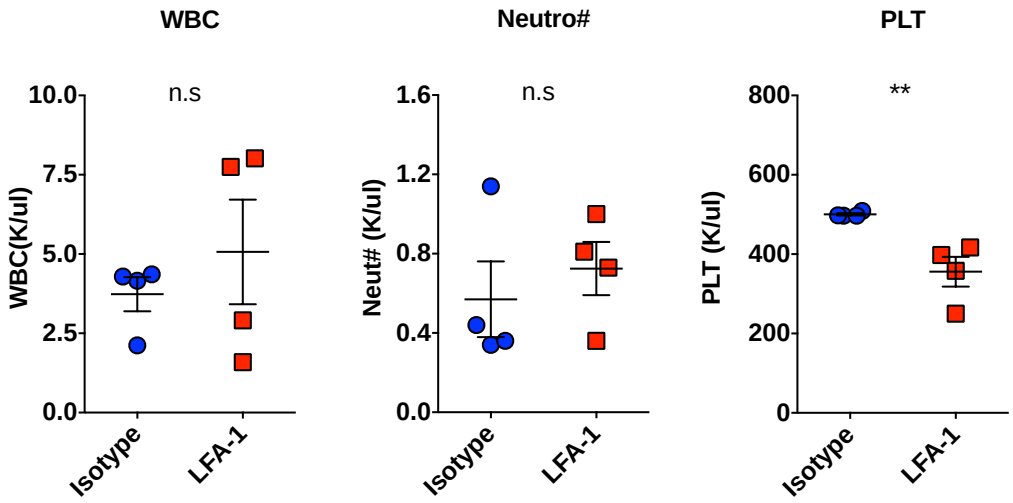

Fig.4.4.2.1 Peripheral blood counts of C57BL/6 mice after received 3

times consecutive LFA-1 antibody blocking

N=4, error bars, mean±SEM **P<0.01, n.s not significant, data representing two independent experiments analyzed with unpaired Student's t-test.

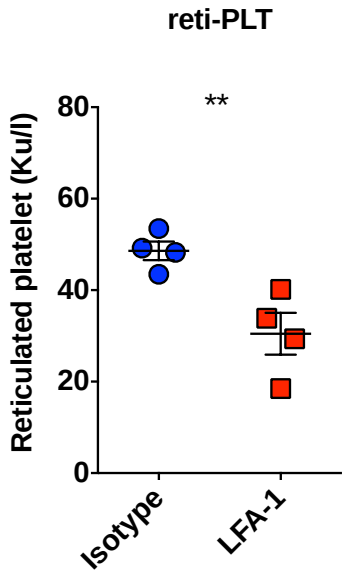

Fig.4.4.2.2 Flow cytometric analysis of reticulated platelets fragments by thiazole orange staining after LFA-1 blocking

N=4 per group, error bars, mean±SEM,**P<0.01, data representing two independent experiments analyzed with unpaired Student's t-test.

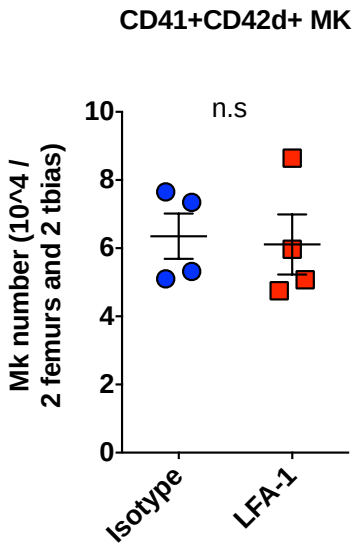

Fig.4.4.2.3 Flow cytometric assessment of mature MK numbers after LFA-1 antibody blocking.

N=4 per group, error bars, mean±SEM n.s non-significant, data representing two independent experiments analyzed with unpaired Student's t-test.

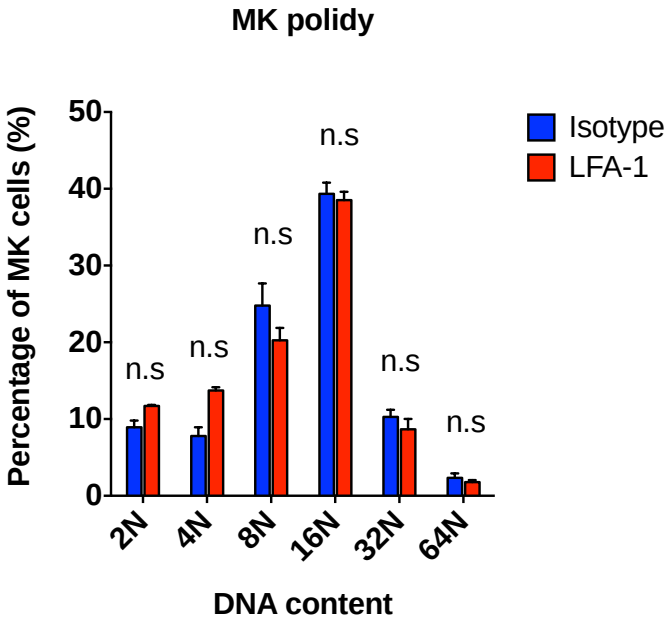

Fig.4.4.2.4 Flow cytometric quantification of MK ploidy after LFA-1

antibody blocking.

N=4 per group, error bars, mean± SEM, n.s not significant, data analyzed with unpaired Student's t-test.

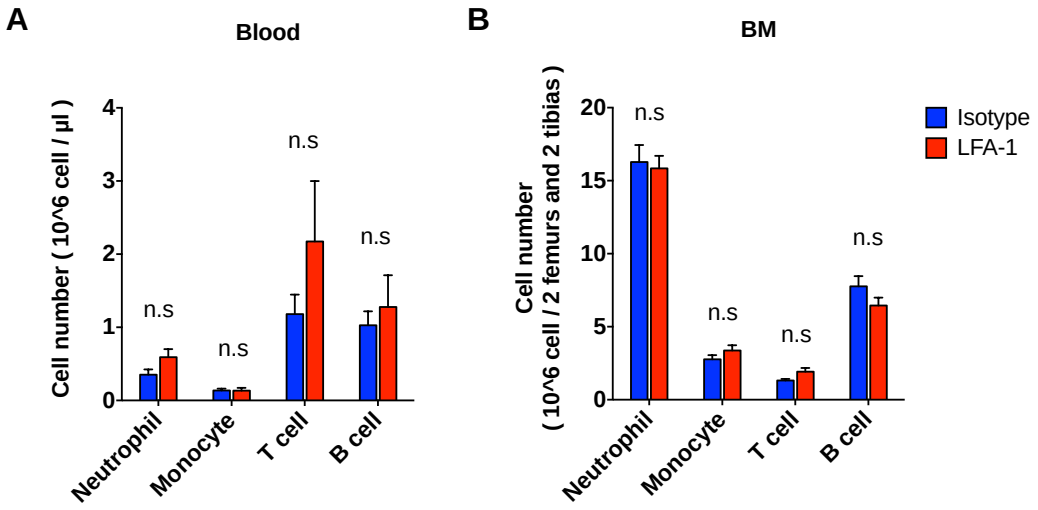

Fig.4.4.2.5 Cellularity and numbers of leukocyte subsets in (A) peripheral blood and (B) bone marrow after LFA-1 blocking

N=4 per group, error bars, mean± SEM n.s not significant, data representing two independent experiments analyzed with One-way ANOVA followed by Tukey's multiple comparison test.

4.5 MK-PMN interactions during thrombopoiesis are SDF-1 dependent

4.5.1 $Mrp8^{cre}$ x $CXCR4^{flox/flox}$ knockout mice show reduced platelet counts

CXCR4/SDF-1 chemokine axis regulates PMN homeostasis within the BM. $Mrp8^{cre}$ x $CXCR4^{flox/flox}$ conditional knockout mice show a neutrophil homing defect due to the absence of CXCR4 on neutrophils yielding a neutrophilic

phenotype. Interestingly, this mouse line exhibited reduced platelet counts in the peripheral blood. Therefore, further investigation of this mouse model may help to decipher the underlying molecular mechanism of our findings.

Peripheral blood counts under steady conditions were measured in Cre- and Cre+ mice as done before (**Fig.4.5.1.1**). Flow cytometry analysis revealed that Cre+ mouse generate less reticulate platelets in comparison to Cre- mice (**Fig.4.5.1.2**). However, platelet clearance was not affected in the absence of CXCR4 removal on neutrophils (**Fig.4.5.1.4**). Furthermore, neither counts of matures, MK maturation (**Fig.4.5.1.3 and Fig.4.5.1.5**) or any other white blood cell population was altered within the peripheral blood or bone marrow (**Fig.4.5.1.6**).

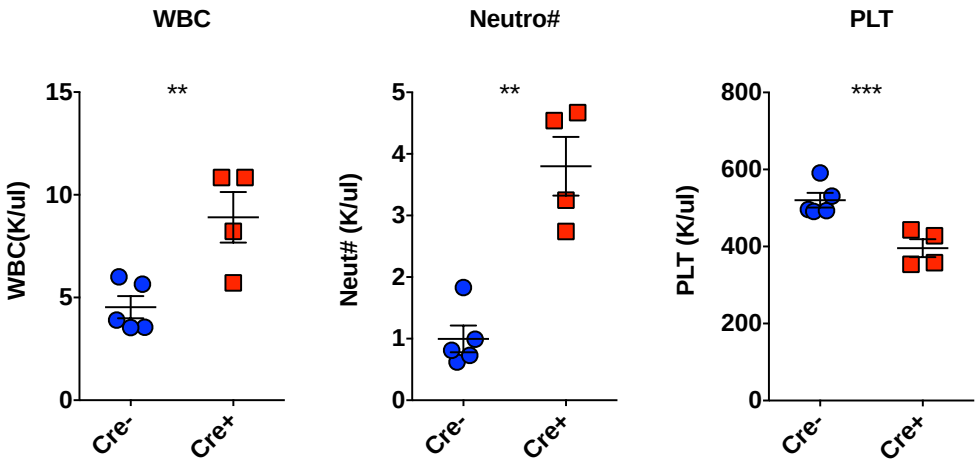

Fig.4.5.1.1 Peripheral blood counts in Mrp8^{cre+} x CXCR4$^{flox/flox}$ and their Mrp8^{cre-} x CXCR4$^{flox/flox}$ littermate controls

N=4-5 per group, error bars, mean±SEM *P<0.05, **P<0.01, ***P<0.001, data was analyzed with unpaired Student's t-test.

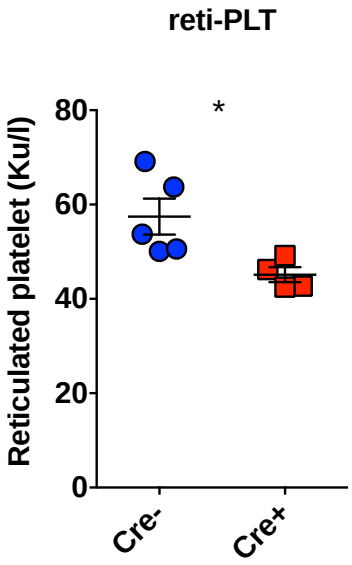

Fig.4.5.1.2 Reticulated platelet fragments assessed by flow cytometry in peripheral blood of Mrp8^{cre} x CXCR4$^{flox/flox}$ mouse line

N=4-5 per group, error bars, mean±SEM *P<0.05, **P<0.01, ***P<0.001, data analyzed with unpaired Student's t-test.

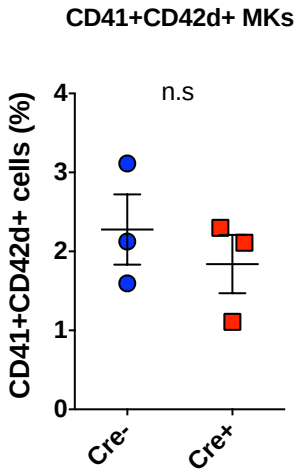

Fig.4.5.1.3 Comparison of mature MKs between Mrp8^{cre+} x CXCR4$^{flox/flox}$ and their Mrp8^{cre-} x CXCR4$^{flox/flox}$ littermate controls

N=3 per group, error bars, mean±SEM. n.s not significant, data was analyzed

with unpaired Student's t-test.

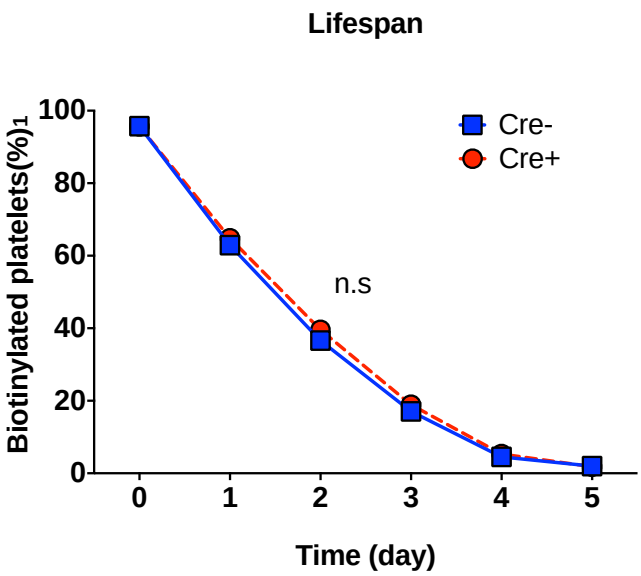

Fig.4.5.1.4 Flow cytometric assessment of platelet lifespan in Mrp8^{cre+} x CXCR4$^{flox/flox}$ and their Mrp8^{cre-} x CXCR4$^{flox/flox}$ littermate controls

N=4, error bars, mean±SEM n.s not significant, data analyzed with paired Student t-test.

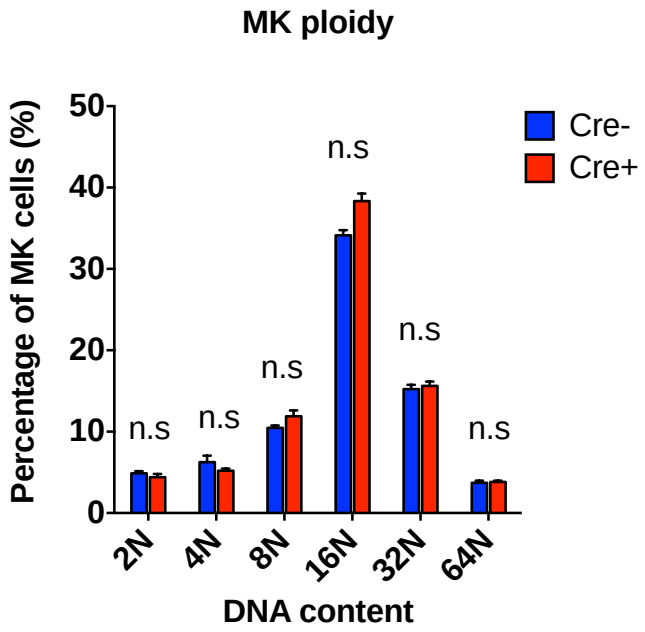

Fig.4.5.1.5 MK ploidy comparison between Mrp8 Cre+ and Mrp8 Cre- mice

N=4 per group, error bars, mean±SEM, n.s non-significant, One-way ANOVA analysis was used for multiple group comparisons.

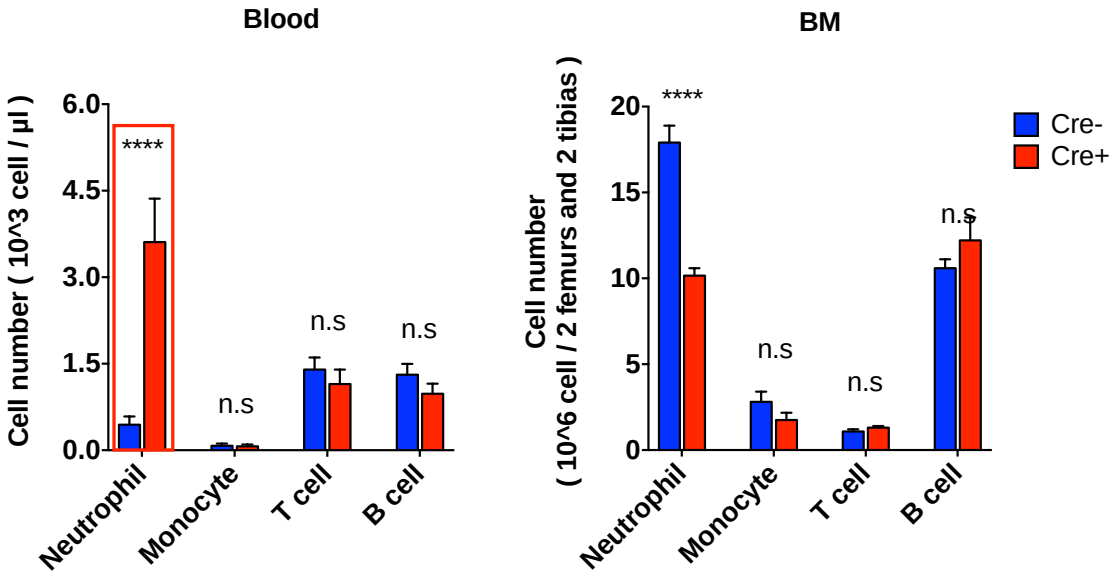

Fig.4.5.1.6 Cellularity and numbers of leukocyte subsets in peripheral blood and BM of Mrp8^{cre+} x CXCR4$^{flox/flox}$ and their Mrp8^{cre-} x CXCR4$^{flox/flox}$ littermate controls

N=3, error bars, mean±SEM, ****P<0.0001, n.s non-significant, One-way ANOVA analysis was used for multiple group comparisons.

4.5.2 MK derived SDF-1 guides PMNs to the bone marrow

Platelets and MKs have been reported as reservoir of SDF-1 but whether MKs are also capable of attracting neutrophils is unknown. Hence, we firstly examined the expression of SDF-1 in the PPF MKs by confocal microscopy. As the representative pictures showed, SDF-1 is highly expressed on

differentiated MKs, in particular on proplatelet shafts. In order to confirm our hypothesis that MKs are able to attract PMNs towards the budding site during the thrombopoiesis, we adoptively transferred 2.5 million PMNs isolated from $Mrp8^{cre+}$ x $CXCR4^{flox/flox}$ LysM eGFP mice and their littermate controls into the normal C57BL/6 mice. One hour later, all mice were sacrificed and perfused with 4% PFA before harvesting the bones. For the staining CD41-PE, CD144 and anti-GFP primary antibodies were used to label the MKs, vessels and transferred neutrophils in the bones, respectively. As shown in Figure **4.5.2.2**, most transferring wildtype PMNs located in proximity to the MKs. However, homed CXCR4 knockout neutrophils were less frequently observed and distributed in random manner. This data strongly suggested that MKs may work as a SDF-1 reservoir like endothelial cells to attract homing neutrophils through the CXCR4-CXCL12 axis signaling pathway in the bone marrow.

Additionally, by live imaging we observed that some neutrophils migrated back to the bone marrow compartments along proplatelets (**Fig.4.5.2.3**) entering in close proximity to the proplatelet budding. Due to the short life span of neutrophils and maintenance the constant number of neutrophils in the peripheral blood, every day neutrophils follow the daily cycles of releasing from and migrating back to the BM when get aged. Hence, these homing neutrophils around the budding sites might be older “aged” neutrophils. Given the higher expression of CXCR4 on the aged neutrophils (Adrover JM, et al. (2019), the aged neutrophils might be a potential regulator during thrombopoiesis.

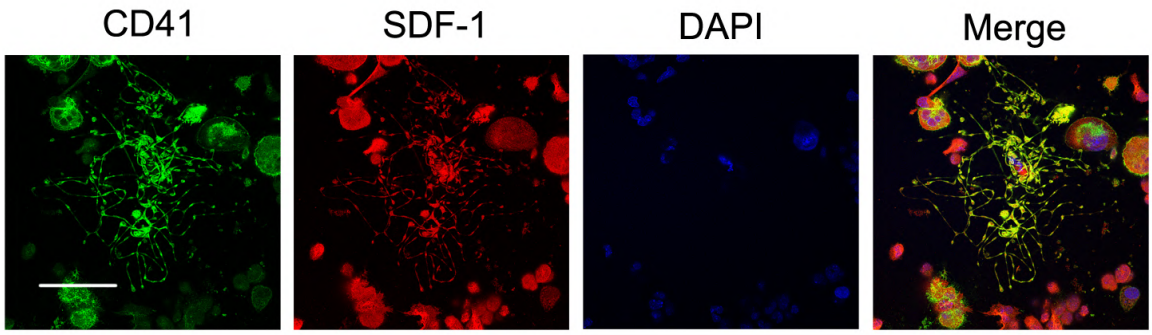

Fig.4.5.2.1 Representative images of SDF-1(red) expression in MKs (green), counterstained DAPI (blue) (scale bar, 20μm)

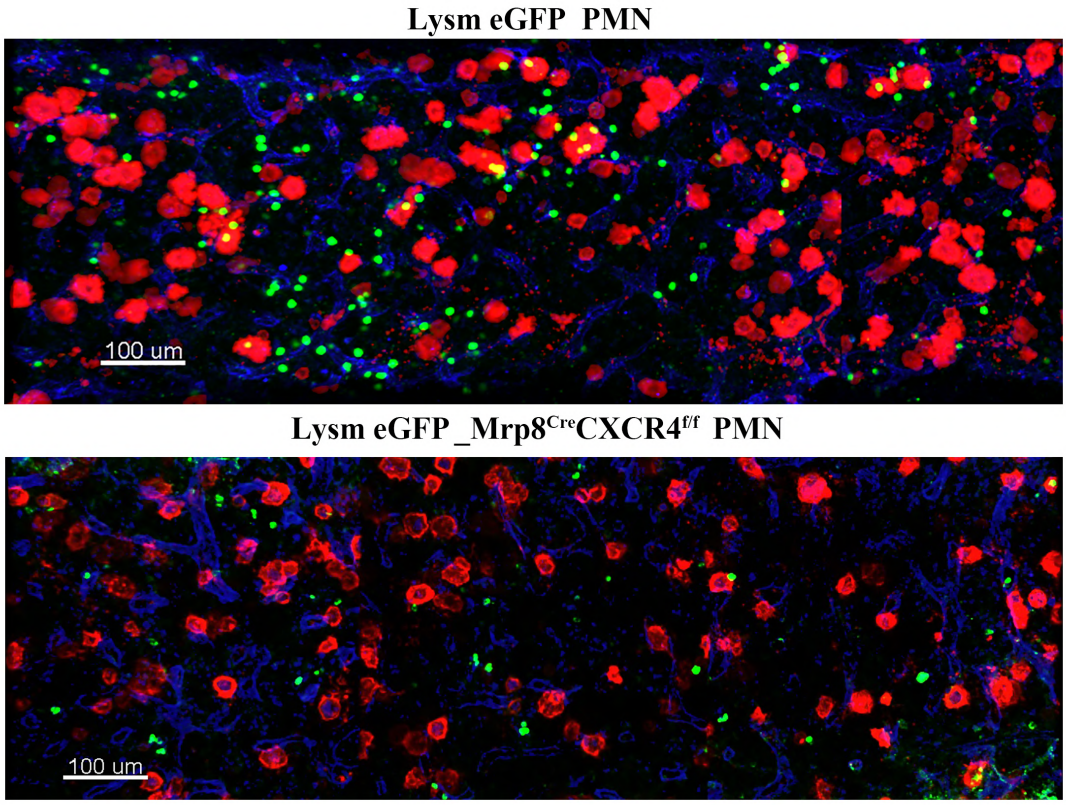

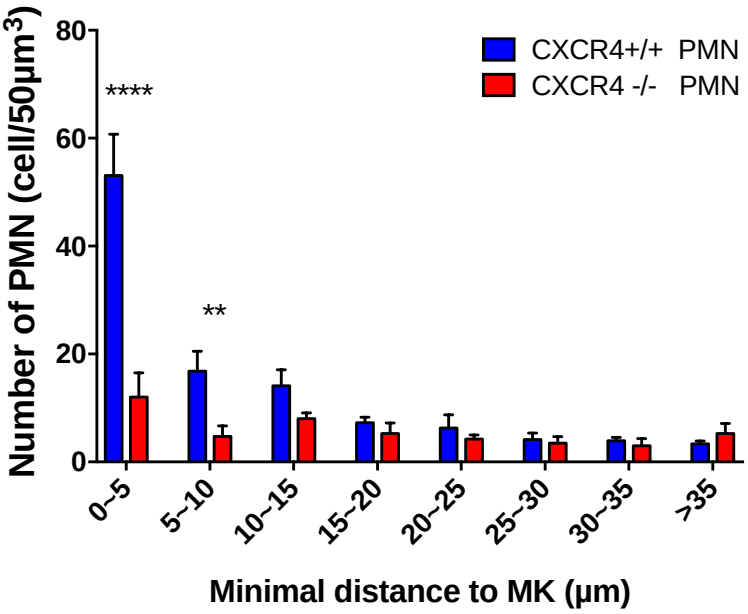

Fig.4.5.2.2 Megakaryocytes attract the PMNs in vivo

(A) Representative whole mount images of PMNs distribution within the BM 1 hour after transfer. CD144(blue), CD41(red), green anti-GFP (green). Scar bar, 100μm. (B) localization of transferring PMNs (CXCR4-/- or CXCR4+/+) relative to MKs (N=4, error bars, mean±SEM, the numbers on the x axes in (B) indicate ranges *P<0.05, **P<0.01, ***P<0.001, data analyzed with One-way ANOVA test).

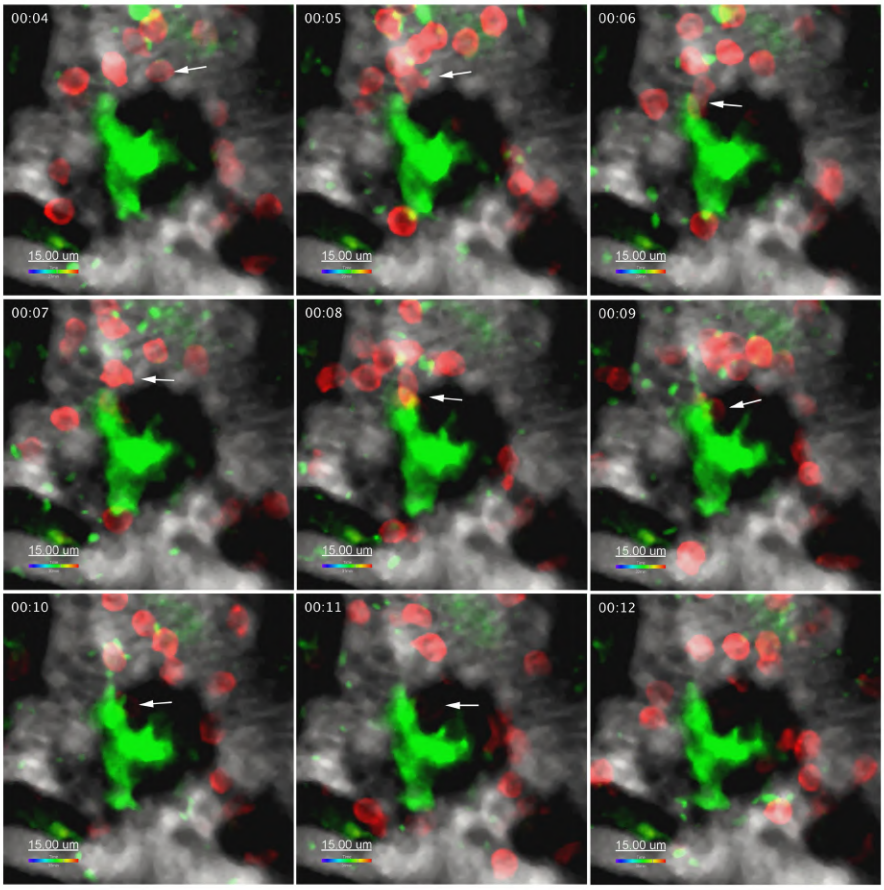

Fig.4.5.2.3 Representative of PMNs extravasating along a protruding proplatelet towards the BM

white arrows indicate the extravasated neutrophils, MKs display green fluorescence, neutrophils and vessel represent red and gray color, respectively. scale bar, 15μm

4.5.3 CXCR4 guide PMNs to the budding site of proplatelets

Using an antibody labeling method (Stegner D. et al. 2017), we visualized the neutrophil and megakaryocyte interactions in the $Mrp8^{cre}$ x $CXCR4^{flox/flox}$ knockout mice. In comparison to the littermate control, $Mrp8^{cre}$ x $CXCR4^{flox/flox}$ knockout mice have higher numbers of neutrophils in the vascular compartment due to the homing defect. CXCR4 knockout mice also displayed

the same phenotypes during thrombopoiesis as we found in the confetti mouse model under neutropenic condition (i.e. prolonged releasing time) (**Fig.4.5.3.1A**). The video analysis also (**Fig.4.5.3.1B**) indicated less PMN-MK interactions appeared around the budding sites of proplatelet forming megakaryocytes within the vascular niche. Additionally, the in vitro analysis of PAF numbers after co-culturing MKs with isolated CXCR4 knockout neutrophils also implies that CXCR4 on the neutrophils was indeed of critical importance for the platelets production in vitro. In summary, we concluded that $Mrp8^{cre}$ x $CXCR4^{flox/flox}$ mice had less platelet counts due to their defects of homing to BM and subsequently avoidance of recruitment by MKs around budding sites.

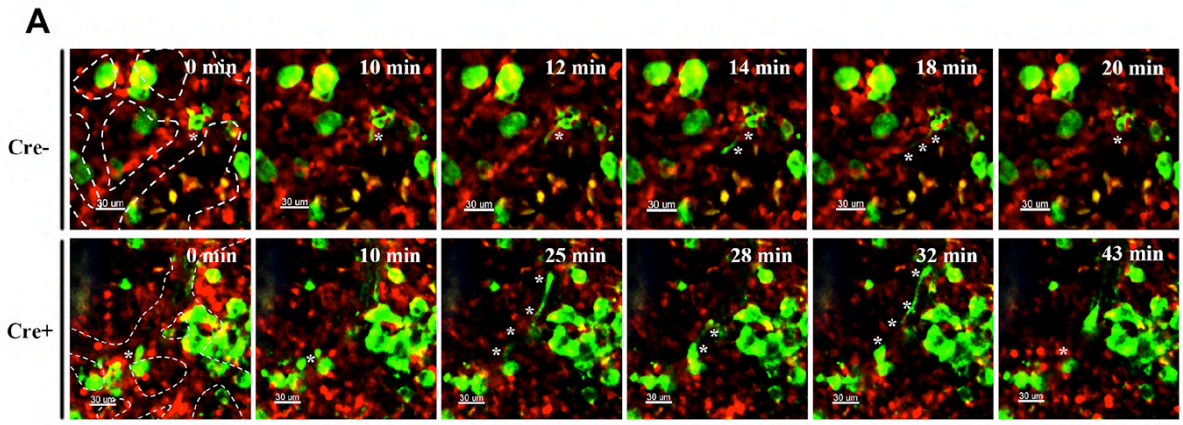

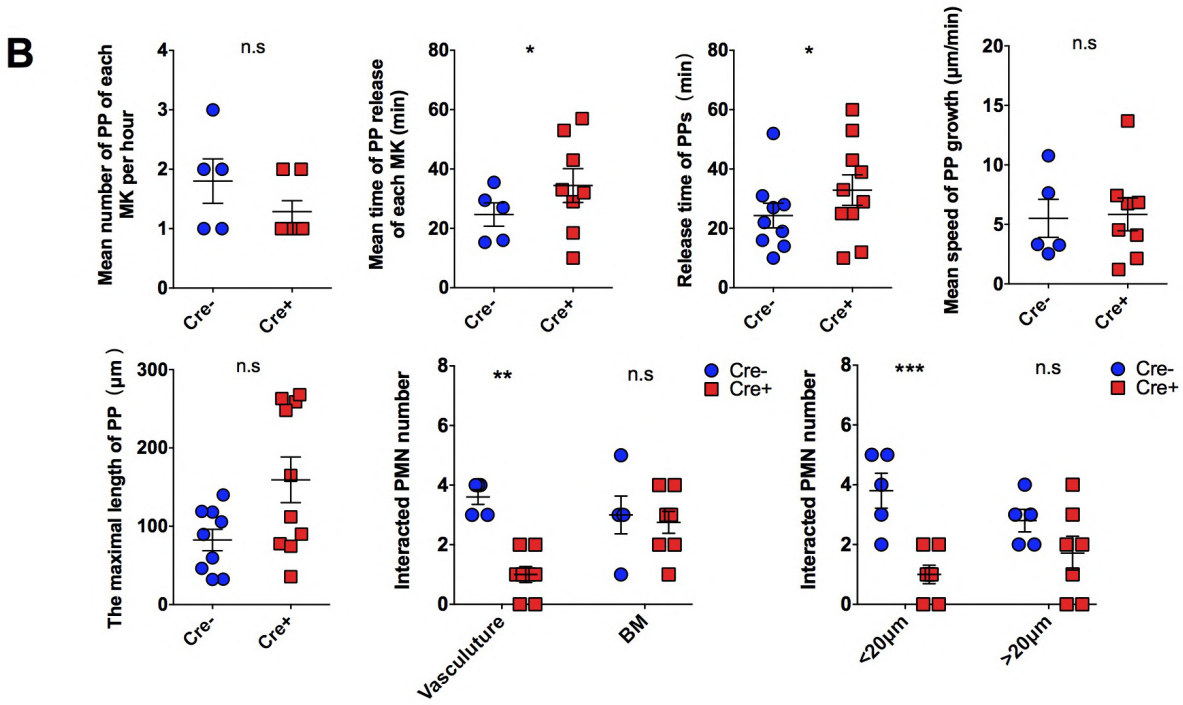

Fig.4.5.3.1 Quantification and assessment of proplatelet formation in Mrp8^{cre} x CXCR4$^{flox/flox}$ mouse model.

(A) representative images of proplatelet forming process in Mrp8^{cre-} x CXCR4$^{flox/flox}$ and their littermate controls; dash line indicate the vessels, scale bar, 30μm (B) Analysis of proplatelet releasing numbers, time, growth speed, and interacted PMN numbers in circulation and bone marrow, etc. N=3, error bars, mean±SEM. Data analyzed with unpaired Student t-test.

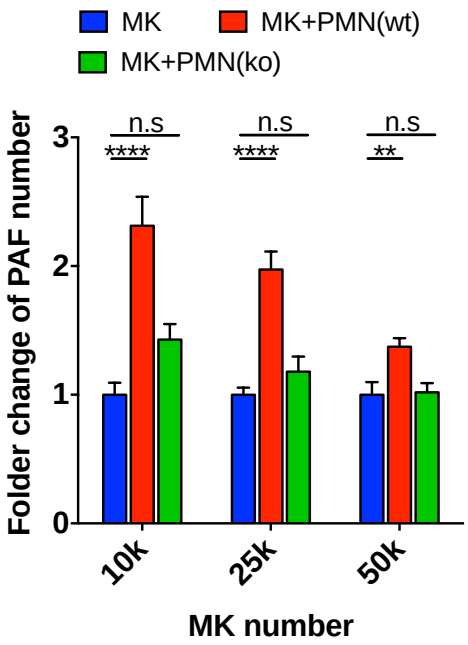

Fig.4.5.3.2 Quantification of PAF number after co-culturing MKs with CXCR4 deficient PMNs

N=3 per group, error bars, mean±SEM **P<0.01, ****P<0.0001, n.s non-significant, data representing 3 independent experiments, One-way ANOVA analysis was used for multiple group comparisons.

4.6 Role of reactive oxygen species (ROS) on thrombopoiesis

4.6.1 Inhibition of NADPH oxidase in neutrophils reduces the PAF generation in vitro

Aged neutrophils do not only show a higher expression of CXCR4, but also have different phenotypic changes in comparison to younger neutrophils (Adrover JM, et al. 2019). Previous studies have reported that reactive oxygen species (ROS) could regulate the differentiation, maturation and even platelet

production of MKs in the BM niches. Additionally, it is widely accepted that neutrophils are a big resource of ROS and recent study reports aged neutrophils exhibit a stronger capacity to produce ROS in comparison to young ones (Adrover JM, et al. 2019). Our previous data has mentioned that homing cells were critical importance of proplatelet forming and shedding. To investigate the role of neutrophil derived ROS during the thrombopoiesis, we were first to use, a broad inhibitor of the NADPH oxidase, apocynin, to block the neutrophil derived ROS and evaluated its effect on PAF production in vitro in our co-culture model. Flow cytometry analysis showed (**Fig.4.6.1.1**), that ROS inhibition in neutrophils blunts the additive effects of neutrophils on PAF. Additionally, $p22^{phox}$ mutated neutrophils (NADPH oxidase defect neutrophils) also showed a same trend (**Fig.4.6.1.2**) after co-culture with MKs. Taken together, these data suggest that ROS produced by neutrophils had a direct effect on platelet biogenesis.

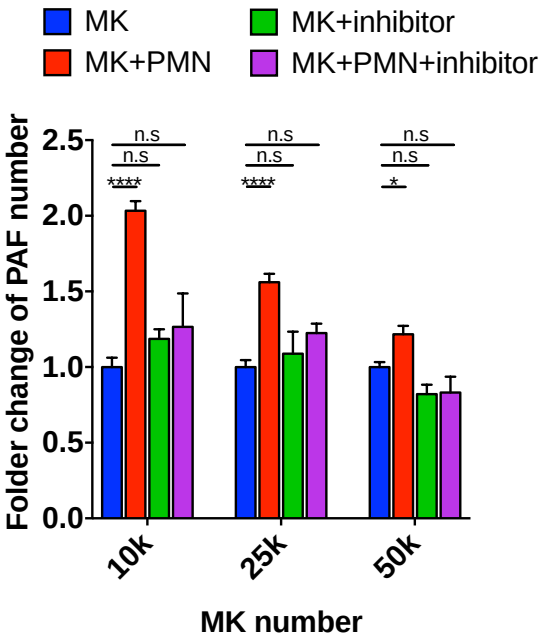

Fig.4.6.1.1 Flow cytometric analyses of PAF counts after co-culture

apocynin inhibited PMNs

PMNs pre-incubated with cytoskeleton protein inhibitors before co-culturing with MKs, N=3 per group, error bars, mean±SEM *P<0.05, ****P<0.0001, data representing 3 independent experiments and One-way ANOVA analysis was used for multiple group comparisons.

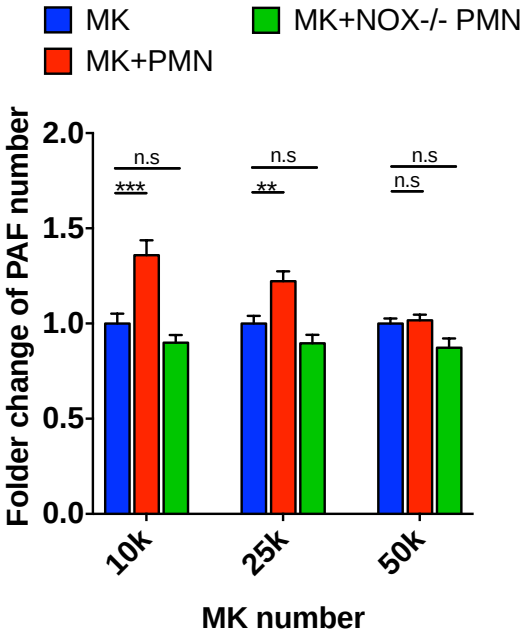

Fig.4.6.1.2 Quantification of PAF number after co-culture MKs with p22^{phox} mutated neutrophils

N=3, error bars, mean±SEM, **P<0.01, ***P<0.001, n.s non-significant, data representing 3 independent experiments analyzed with One-way ANOVA followed by Tukey's multiple comparison test.

4.7 Circadian rhythm of platelets counts

4.7.1 Platelets count oscillation regulated by circulating neutrophils

Even though we demonstrated that neutrophils augment platelet counts by interacting with MKs and releasing ROS molecules, the physiological relevance of this phenomenon is still elusive. Oscillation of neutrophil counts over the day seems to play a protective role in some cardiovascular diseases (i.e. myocardial infarction) (Adrover JM, et al. 2019). Previous studies reported that neutrophils numbers within circulation reach a peak at ZT5 (zeitgeber time 5, 5 hours after light on) and a nadir at ZT13, respectively (María Casanova-Acebes, et al., 2013).

Our findings indicated that MK-PMN interactions drive thrombopoiesis hence we addressed whether the number of circulating neutrophil affects platelet counts over the day. Hence, we evaluated platelet counts of a day at ZT5 and ZT13, respectively. Interestingly, platelet counts also presented a similar oscillation like neutrophils over the day (**Fig.4.7.1.1**). At ZT5, platelet and reticulated platelet counts were higher than those at ZT13. Among all observed leucocyte and lymphocyte populations only circulating neutrophils showed a circadian rhythm, suggesting that these circulating neutrophils may drive the oscillation of platelets in vivo.

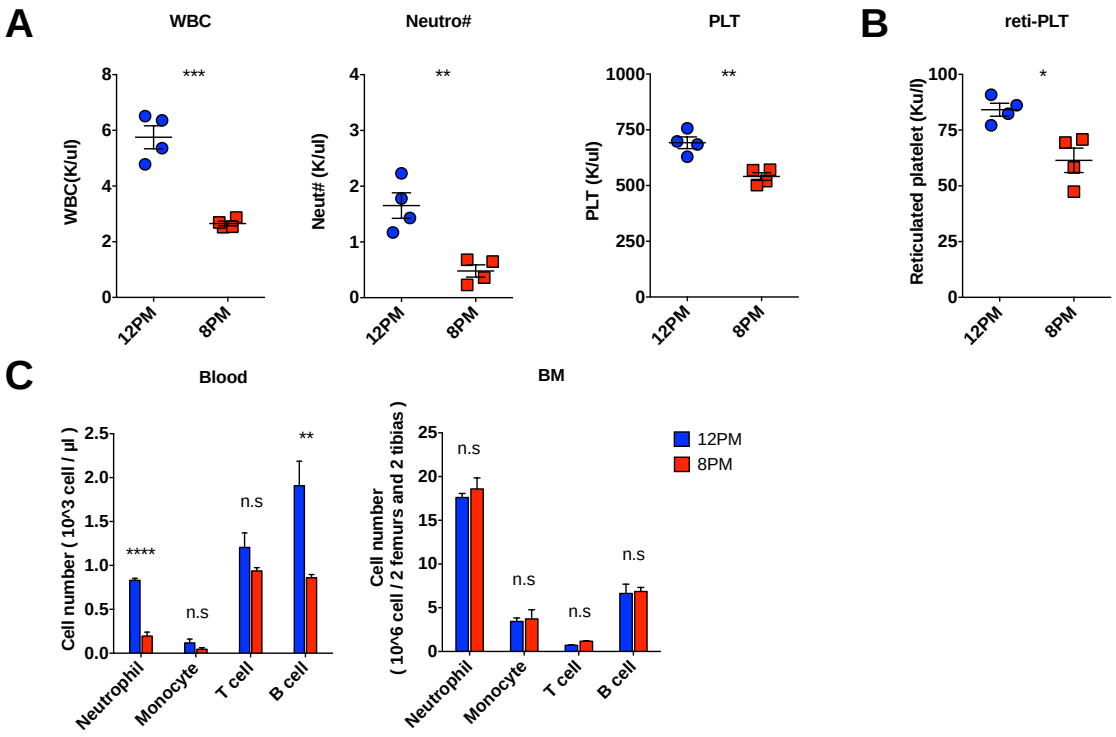

Fig.4.7.1.1 Circulating neutrophils regulate the platelet oscillation.

(A) Blood counts of wildtype mice at ZT5 and ZT13, respectively. (B) Reticulated platelets were stained by thiazole orange and analyzed by flow cytometry at ZT5 and ZT13, respectively. (C) Blood and bone marrow, cellularity and number quantification of leukocyte subsets at ZT5 and ZT13, respectively N=4 male mice per group, error bars, mean±SEM *P<0.05, **P<0.01, ***P<0.001, ****P<0.0001,n.s nonsignificant, data representing two independent experiments analyzed with unpaired Student's t-test.

4.7.2 Oscillation of platelet counts depends on ICAM-1 and neutrophil expressed CXCR4

To further investigate whether the same molecular mechanism of MK-PMN interaction contributes to platelet counts oscillation we took advantage of our

ICAM-1 blocking mouse model and Mrp8^{cre} x CXCR4$^{flox/flox}$ knockout mouse model. As above mentioned, ICAM-1 blocking or removal of CXCR4 on neutrophils would affect the platelet production due to the homing defect and avoidance of recruitment of homing neutrophils around budding sites. Interestingly, circadian modulation of platelet counts was blunted in both models (**Fig.4.7.1.1**) underscoring the close interdependency of platelet form PMN counts.

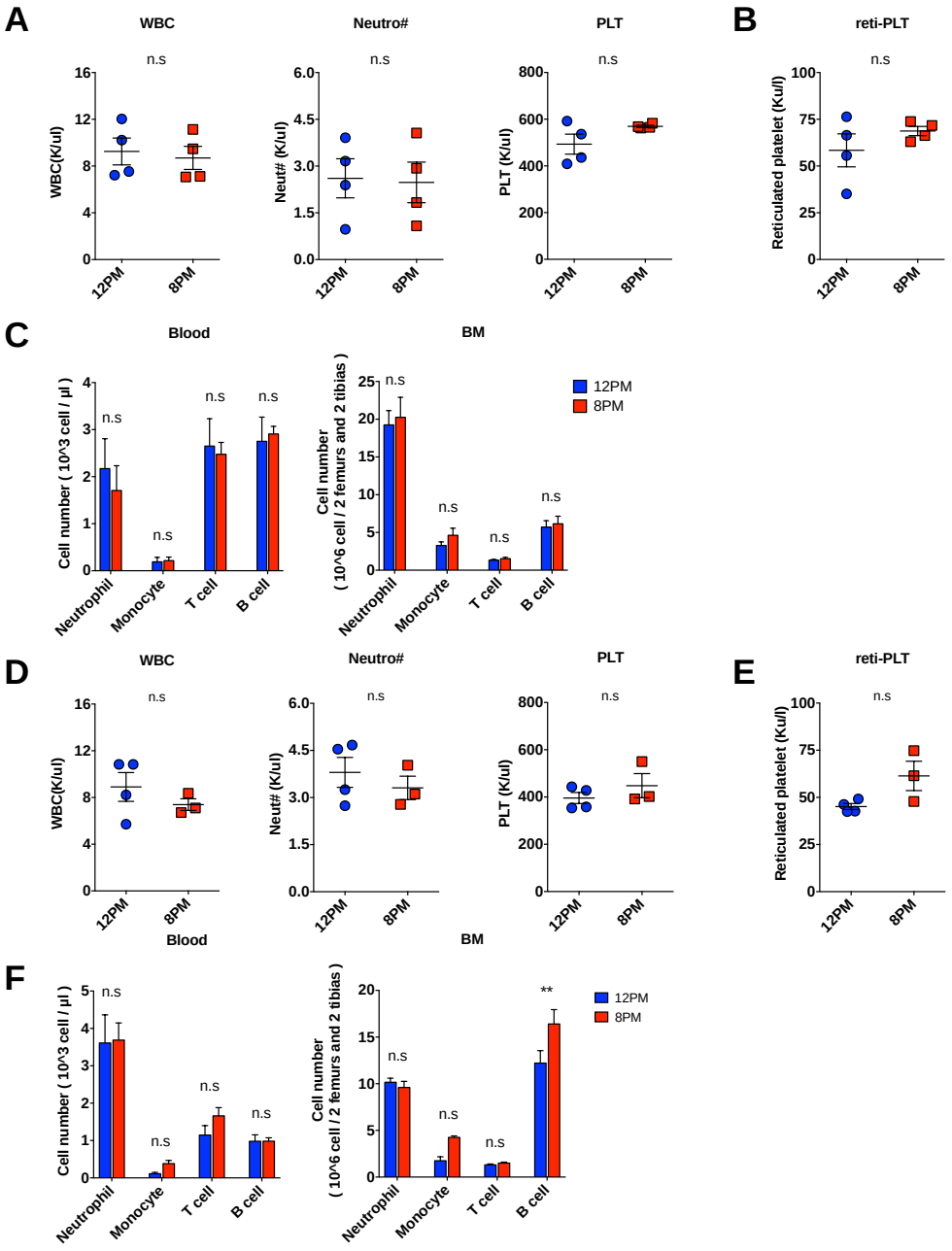

Fig.4.7.2.1 Platelet oscillation disappear in the LFA-1 blocked mice or Mrp8^{cre+} x CXCR4$^{flox/flox}$ mice

(A)peripheral blood counts of LFA-1 blocked mice measured at ZT5 and ZT13, respectively. B. quantification of reticulated platelets fragment at ZT5 and ZT13, respectively. (C). Blood and bone marrow cellularity and numbers of leukocytes subpopulations in LFA-1 blocked mice (D) peripheral blood counts of Mrp8^{cre}_CXCR4$^{flox/flox}$ knockout mice at ZT5 and ZT13, respectively. (E) Reticulated platelet counts at ZT5 and ZT13, respectively (F) Blood and bone marrow cellularity and leucocyte subsets numbers at ZT5 and ZT13, respectively (N=4 male mice per group, error bars, mean±SEM, n.s not significant, data representing two independent experiments analyzed with unpaired Student's t-test).

Discussion

Within the last decades several mechanisms were identified that regulate thrombopoiesis under steady state or inflammatory conditions including sphingosine 1-phosphate, IL-1alpha, and CCL5. However, the role of the cellular microenvironment on proplatelet formation and release is still poorly understood. In this study we provide evidence that homing aged neutrophils promote proplatelet shedding through generation of ROS molecules.

Our findings demonstrate that a long time depletion of neutrophils in a conditional knockout mouse model (Rosa26^{iDTR} x Mrp8^{Cre} mouse) can attenuate platelet production and subsequently reduce platelet counts by 30% compared to controls. However, even though neutrophils are completely eliminated through diphtheria toxin receptor-mediated conditional ablation, platelet counts only showed a one-third decrease with no additional effect after 5 days of treatment. A previous study (Laurent L. Reber et al., 2017) reported that a single treatment of Rosa26^{iDTR} x Mrp8^{Cre} mice with diphtheria toxin also leads to a slight but not significant decrease of thrombocytes possibly due to sex and age differences between the mice. However, thrombopoiesis was not completely diminished in the absence of neutrophils. Likewise, Ly6G/C antibody mediated neutrophil depletion in C57BL/6 wildtype mice also yielded reduced platelet counts (around 25% and 33% reduction at day 3 and day 5, respectively) over time. Importantly, both neutropenic mouse models did not show an alteration in the number or maturation (i.e. ploidy) of CD41+CD42d+ megakaryocytes, indicating that neutrophil depletion did not affect megakaryopoiesis but rather influences the level of thrombopoiesis. This is in line with our finding that the fraction of reticulated platelets is reduced under neutropenia, whereas platelet lifespan and clearance are not altered. In summary, these data show that neutrophils primarily regulate platelet

production, not the clearance.

A second key finding of our study is that neutrophils within the vascular compartment play the predominant role during the thrombopoiesis. The bone marrow interstitium and vasculature are the two main neutrophil pools. The bone marrow interstitium serves as a site of neutrophils production and clearance to maintain the cellular homeostasis and immunity balance by chemokine signaling communications (María Casanova-Acebes, et al., 2013). The circulating pool within the vasculature that predominantly consists of mature and aged neutrophils represents innate immunity to maintain body integrity and to tackle invading pathogens (Charlotte Summers, et al., 2010.) Indeed, the vascular pool mediates the effects on thrombopoiesis, given that we did not observe an additional effect in our iDTR neutropenic model that depletes both PMN pools in contrast to the antibody depletion model that only reduces the intravascular pool.

Using multiphoton intravital microscopy, we were first to visualize physical interactions between neutrophils and megakaryocytes. Importantly these interactions occur within the BM interstitium as well as the vascular compartment. However, using sphericity index to categorize MKs, we observed a different interaction dynamic in highly differentiated MKs (low sphericity index) with a high capacity to form proplatelets: they establish more and longer lasting interactions with PMNs compared to less proliferative MKs (high sphericity index). To further characterize MK-PMN interaction during platelet production we visualized proplatelet formation within the BM in the presence and absence of neutrophils in two fluorescent reporter gene mouse models. Our data from the antibody depletion experiments reveals that MK-PMN interactions within the bone marrow niche do not change before and after depletion. Worthy of note, no interaction can be found within the vasculature. On the basis of this knowledge we observed attenuated

proplatelet formation speeds and prolonged shedding times, but no changes concerning the proplatelet lengths, underscoring the importance of PMNs within the bloodstream.

By quantifying distances from interacting PMNs to proplatelet budding sites our data suggest that PMN residing in close proximity to the budding site (<20µm) play the dominant role on proplatelet formation and shedding.

Given the intrinsic limitations to study MK-PMN interactions and its molecular basis in vivo we established an in vitro co-culture model. Hence, we were able to investigate whether a direct physical interaction or paracrine signaling events drive proplatelet formation and shedding. A borden chamber based in vitro co-culture assay indicates physical interaction is indispensable for this neutrophil mediated platelet biogenesis. Furthermore, cytokines released by activated PMNs likewise showed the paracrine signaling events are not of critical importance to augment the proplatelet forming and shedding in vitro.

MK-PMN interactions are preceded PMN endothelial cell interactions, we found that ICAM-1 blocking yields reduced platelet counts as seen before in the absence of intravascular PMN. Additionally, Efalizumab, a monoclonal ICAM-1 blocking antibody, no longer clinically available due to sporadic but deadly severe infections, induced thrombocytopenia as a common side effect in patients (Hostetler SG, et al. 2007). Taken together, our data show that the intravascular, vessel wall adherent pool of PMNs that localize in proximity to the proplatelet budding site drive thrombopoiesis.

Next, we aimed to identify the mechanism that triggers PMN recruitment to proplatelet budding sites. Previous studies have demonstrated that platelets resemble a reservoir of SDF-1alpha, and also MKs are capable of secreting CXCL12 (Steffen Massberg, et al. 2006). Further it was shown that the CXCR4/SDF-1 chemokine axis regulates PMN homeostasis within the BM.

Mature and activated neutrophils accompany with increased SDF-1 induced calcium influx and higher CXCR4 expression. Neutralization by low dose CXCR4 antibody reduces the neutrophils sequestration and retention in the BM (Suratt BT, et al. 2004). Hence, megakaryocyte derived CXCL12 mediates the neutrophil recruitment to megakaryocytes, additionally, especially aged neutrophils that home back to the BM highly express CXCR4 (Casanova-Acebes, et al. 2013). Hence the removal of CXCR4 on neutrophils in mice leads to leukocytosis due to a defect of the neutrophils homing capacity. Interestingly, this mouse model shows reduced platelet counts, as seen before in the absence of PMN, underscoring the importance of the neutrophils CXCR4 expression on platelet biogenesis. But what are the links between them? In vivo visualization revealed that the removal of CXCR4 on the neutrophils leads to decreased neutrophil interactions within the vascular niche. This is in line with our hypothesis that neutrophil recruitment to proplatelet forming MKs drives thrombopoiesis. Previous studies have demonstrated that CXCL12 can be released by endothelial cells and regulate the lineage biased HSCs distribution in vivo (Sandra Pinho, et al. 2018). Hence, we sought to determine whether MKs or endothelial cells dominated the attraction of attached neutrophils to MKs in the circulation. Adoptively transferred neutrophil experiments revealed that the removal of CXCR4 on neutrophils leads to a random distribution of neutrophils within the bone marrow niche, whereas wildtype neutrophils showed a specific MK-orientated distribution. This finding suggests that the homing of aged neutrophils might be extrinsically driven by endothelial cells and MKs together. In addition to endothelial cells in bones, MKs might be another source of CXCL12 that mediates cell migration and distribution in the bone marrow niche.

Neutrophils originate from myeloid biased HSCs within the bone marrow and are released into circulation to provide an early immunity protection

against the pathogens. Due to their short lifespan (approximately 5~6 hours) neutrophils are continuously produced in the bone marrow and cleared in specialized organs (i.e. bone marrow, liver) by phagocytes to maintain a constant number in the bloodstream. This production-clearance dynamic entails a good balance between the release of young neutrophils and the clearance of aged ones. The young neutrophils transformation into aged ones implies not merely the phenotypic changes, but moreover the functional diversification. In contrast to young neutrophils, aged neutrophils are smaller and less granular. Murine neutrophils present increased CXCR4 but reduced CD62L (also known L-selectin) expression while in the circulation. Transcriptomic analyses show that aged neutrophils exhibit many pro-inflammatory genes (i.e. TNF-α) as neutrophils are activated by inflammatory stimuli throughout their time in the circulation. Further studies demonstrated that aged neutrophils favor a pro-inflammatory phenotype (i.e. NETosis formation) that predisposes to vascular inflammation (i.e. myocardial infarction) (Adrover JM, et al. 2019). Under inflammatory conditions activation of integrins or G-protein-coupled receptors on neutrophils triggers the production of reactive oxidative species (ROS) to subsequently activate proteinases (i.e. Myeloperoxidase) and to form extracellular NETs (Nguyen GT, et al. 2017). In this context, aged neutrophils were found to generate increased amounts of ROS than “fresh” neutrophils (Adrover JM, et al. 2019). ROS is known to regulate the HSCs proliferation, differentiation, as well as MKs maturation (Chen S, Su Y, Wang J. 2013). In addition, a lipid mediator, 15-Deoxy-D12,14-PGJ2, was shown to directly influence platelet release through promotion of the redox state in the MKs and change of the cellular cytoskeleton. This finding indicates that the platelet biogenesis process can be directly influenced by ROS molecules (O’Brien JJ, et al. 2008). In our setting we used apocynin, a global NADPH oxidase inhibitor, to blunt ROS production

within neutrophils that would recede the effect of platelet production by neutrophils in vitro, Likewise, a co-culture of MKs with neutrophils isolated from the NADPH oxidase mutated mice ($p22^{phox}$ mutation mice) also proved that proplatelets formation was neutrophil-derived-ROS dependent. Additionally, $p22^{phox}$ mutation mice similarly displayed a thrombocytopenic phenotype and a decrease in the generation of reticulated platelets (data not shown). Due to a global $p22^{phox}$ mutation in this mouse line, the role of other ROS producing cell types, in particular endothelial cell, are difficult to exclude. Nevertheless, we still could conclude that ROS is of critical importance for the platelet biogenesis in vivo.

Aged neutrophils exhibit an intrinsic circadian oscillation to meet the various diurnal challenges. In the model of acute myocardial infarction the extent of the myocardial damage displays a diurnal variation, and infarct size exhibits a strong negative correlation with the number of aged neutrophils in the circulation, indicating that aged neutrophils play a protective role in tissues after ischemia/ reperfusion (Adrover JM, et al. 2019). In analogy we and others found that platelet counts and their functions vary over the day. In addition, husbandry conditions impact on this oscillation to some extent (Hartley PS. 2013). Nevertheless, the underlying mechanisms that regulate this variation in platelet counts remain obscure. However, our data uncovered that neutrophil and platelet counts oscillate in the same phase, an effect that can be abolished by interfering with PMN homing to the BM after ICAM-1 block or in the absence of CXCR4 on neutrophils. Interestingly, the fluctuating platelet counts accounted for about 30% of total platelets in the mice analogous to the platelet number at ZT5 and ZT13, respectively.

Taken together, our study identified aged PMN as drivers of thrombopoiesis by releasing ROS. This newly identified mechanism that regulates platelet production provides a new direct link between the innate

immune system and primary hemostasis, two closely linked mechanisms. The suggested mechanism resembles a new fast and direct way to govern different platelet demands under conditions of increased platelet demands as found in various physiological and pathological conditions (i.e. trauma) (N. Valade, et al. 2005).

Hence our findings do not merely give insight into a novel concept of platelet biogenesis involving the interaction between MKs with other immune cells, it also uncovers a new function for homing neutrophils.

Reference

Althaus K & Greinacher A. (2009) MYH9-related platelet disorders. Semin Thromb Hemost. 35(2):189-203.

Avci Z, et al. (2002) Thrombocytopenia and emperipolesis in a patient with hepatitis an infection. Pediatr Hematol Oncol. 19(1):67-70.

Adrover JM, et al. (2019) A Neutrophil Timer Coordinates Immune Defense and Vascular Protection.Immunity. 50(2):390-402.e10.

Bennett JS. (2005) Structure and function of the platelet integrin alphaIIbbeta3. J Clin Invest 115:3363–3369.36.

Benjamin T Kile, (2015) Aging platelets stimulate TPO production. Nat Med. 21(1):11-2

Bobik R, Dabrowski Z.(1995) Emperipolesis of marrow cells within megakaryocytes in the bone marrow of sublethally irradiated mice. Ann Hematol. 70(2):91-5.

Broudy VC, et al. (1995) Thrombopoietin (c-mpl ligand) acts synergistically with erythropoietin, stem cell factor, and interleukin-11 to enhance murine megakaryocyte colony growth and increases megakaryocyte ploidy in vitro. Blood. 85(7):1719-26.

Bruns I. et al. (2104) Megakaryocytes regulate hematopoietic stem cell quiescence through CXCL4 secretion.Nat Med. 20(11):1315-20.

Bluteau D, et al. (2012) Dysmegakaryopoiesis of FPD/AML pedigrees with constitutional RUNX1 mutations is linked to myosin II deregulated expression. Blood. 120(13):2708-18

Branzk N, et al. (2014) Neutrophils sense microbe size and selectively release neutrophil extracellular traps in response to large pathogens. Nat Immunol.

15(11):1017-25.

Carolien M. Woolthuis & Christopher Y. Park (2016) Hematopoietic stem/progenitor cell commitment to the megakaryocyte lineage. Blood. 127(10):1242-8.

Caudrillier A, et al. (2012) Platelets induce neutrophil extracellular traps in transfusion-related acute lung injury. J Clin Invest 122:2661–2671

Carestia A, et al. (2016) Mediators and molecular pathways involved in the regulation of neutrophil extracellular trap formation mediated by activated platelets. J Leukoc Biol 99:153–162

Casanova-Acebes, et al. (2013) Rhythmic modulation of the hematopoietic niche through neutrophil clearance. Cell 153, 1025–1035.

Choi, E.S., et. al. (1995) Platelets generated in vitro from proplatelet-displaying human megakaryocytes are functional. Blood, 85, 402–413.

Chen, Z., et al., (2007) The May-Hegglin anomaly gene MYH9 is a negative regulator of platelet biogenesis modulated by the Rho-ROCK pathway. Blood. 110:171–179.

Chen S, Su Y, Wang J. (2013) ROS-mediated platelet generation: a microenvironment-dependent manner for megakaryocyte proliferation, differentiation, and maturation. Cell Death Dis. 4: e722.

Chang, Y., et al. (2007) Proplatelet formation is regulated by the Rho/ROCK pathway. Blood. 109:4229–4236.

Claudia Momo, et al. (2014) Morphological Changes in the Bone Marrow of the Dogs with Visceral Leishmaniasis. Vet Med Int. 2014: 15058

Crispino, J.D. (2005) GATA-1 in normal and malignant hematopoiesis. Semin. Cell Dev. Biol. 16:137–147.

Czaikoski PG, et al. (2016) Neutrophil extracellular traps induce organ damage during experimental and clinical sepsis. PLoS ONE 11: e0148142

Cangelosi JJ, et al. (2011) Cutaneous Rosai-Dorfman disease with increased number of eosinophils: coincidence or histologic variant? Arch Pathol Lab Med. 135(12):1597-600.

Deutsch VR, Tomer A. (2013) Advances in megakaryocytopoiesis and thrombopoiesis: from bench to bedside. Br J Haematol. 161:778-93.

Engel C, et. al. (1999) Endogenous thrombopoietin serum levels during multicycle chemotherapy. Br J Haematol. 105(3):832-8

Etulain J, et al. (2015) P-selectin promotes neutrophil extracellular trap formation in mice. Blood 126:242–246

Eto K, Kunishima S. (2016) Linkage between the mechanisms of thrombocytopenia and thrombopoiesis. Blood. 127(10):1234-41.

Faust N, et al. (2000) Insertion of enhanced green fluorescent protein into the lysozyme gene creates mice with green fluorescent granulocytes and macrophages. Blood. 96(2):719-26

Freson, K., et al. (2005) The TUBB1 Q43P functional polymorphism reduces the risk of cardiovascular disease in men by modulating platelet function and structure. Blood. 106:2356–2362.

Gawaz M, et al. (1995) Platelet activation and interaction with leucocytes in patients with sepsis or multiple organ failure. Eur J Clin Investig 25:843–851

Gabriele Zuchtriegel, et al. (2016) Platelets Guide Leukocytes to Their Sites of Extravasation. PLoS Biol. 14(5): e1002459.

Gould TJ, Lysov Z, Liaw PC (2015) Extracellular DNA and histones: double-edged swords in immunothrombosis. J Thromb Haemost 13(Suppl 1): S82–S91

Gresele P, et al. (1993) Altered platelet function associated with the bronchial hyperresponsiveness accompanying nocturnal asthma. J Allergy Clin Immunol 91:894–902

Haas S, et al. (2015) Inflammation-Induced Emergency Megakaryopoiesis Driven by Hematopoietic Stem Cell-like Megakaryocyte Progenitors. Cell Stem Cell. 17(4):422-34.

Hamburger SA, McEver RP (1990) GMP-140 mediates adhesion of stimulated platelets to neutrophils. Blood 75:550–554

Humble, J.G., et. al. (1956) Biological interaction between lymphocytes and other cells. Br J Haematol. 2, 283-294.

Hostetler SG, et al. (2007). Efalizumab-associated thrombocytopenia. J Am Acad Dermatol. 57(4):707-10.

Hartley PS. (2013) Mice housed in groups of 4-6 exhibit a diurnal surge in their platelet count. Platelets 24(5):412-4.

Ito, T.et. Al. (1996) Recombinant human c-Mpl ligand is not a direct stimulator of proplatelet formation in mature human megakaryocytes. Br J Haematol. 94(2):387-90.

Italiano, J.E.,et al. (1999) Blood platelets are assembled principally at the ends of proplatelet processes produced by differentiated megakaryocytes. J. Cell Biol. 147:1299–1312.

Junt, T., et al. (2007) Dynamic visualization of thrombopoiesis within bone marrow. Science. 317, 1767-1770.

Jonathan N. Thon, et al. (2010) Cytoskeletal mechanics of proplatelet maturation and platelet release. J Cell Biol.191(4):861-74.

Jenne CN, et al. (2013) Neutrophils recruited to sites of infection protect from virus challenge by releasing neutrophil extra- cellular traps. Cell Host Microbe

13:169–180

Knight Tristan, et al. (2018) Megakaryocytic Emperipolesis in an Adolescent with Hodgkin Lymphoma. J Pediatr Hematol Oncol. 40(4):306.

Kaser, A., et al. (2001) Interleukin-6 stimulates thrombopoiesis through thrombopoietin: role in inflammatory thrombocytosis. Blood. 98:2720–2725.

Kroemer G, Perfettini JL. (2014) Entosis, a key player in cancer cell competition. Cell Res. 24:1280–1.

Kenneth Kaushansky. (2005) The molecular mechanisms that control thrombopoiesis. J Clin Invest. 115(12): 3339–3347

Kellie R. Machlus, et al. (2016) CCL5 derived from platelets increases megakaryocyte proplatelet formation. Blood 127(7): 921–926.

Kaushansky K. (2008) Historical review: megakaryopoiesis and thrombopoiesis. Blood 111(3):981-6.

Kunisaki Y, et al. (2013) Arteriolar niches maintain haematopoietic stem cell quiescence. Nature. 502(7473):637-43.

Lee WB, et. al. (1999) Emperipolesis of erythroblasts within Kupffer cells during hepatic hemopoiesis in human fetus. Anat Rec. 256(2):158-64.

Long, M.W., Williams, N. & Ebbe, S. (1982) Immature megakaryocytes in the mouse: physical characteristics, cell cycle status, and in vitro responsiveness to thrombopoietic stimulatory factor. Blood, 59, 569–575.

Lefrançais E, et. Al. (2017) The lung is a site of platelet biogenesis and a reservoir for haematopoietic progenitors. Nature. 544(7648):105-109.

Livet J; et al. (2007) Transgenic strategies for combinatorial expression of fluorescent proteins in the nervous system. Nature 450(7166):56-62

Machlus, K.R. & Italiano, J.E. Jr (2013) The incredible journey: from

megakaryocyte development to platelet formation. Journal of Cell Biology, 201, 785–796.

Martinod K, Wagner DD (2014) Thrombosis: tangled up in NETs. Blood 123:2768–2776

Malara A, et al. (2015) The secret life of a megakaryocyte: emerging roles in bone marrow homeostasis control. Cell Mol Life Sci. 72(8):1517-36.

Moore KL, et al. (1995) P-selectin glycoprotein ligand-1 mediates rolling of human neutrophils on P- selectin. J Cell Biol 128:661–671

Nakazawa D, et al. (2017) Histones and neutrophil extracellular traps enhance tubular necrosis and remote organ injury in ischemic AKI. J Am Soc Nephrol 28:1753–1768

Nidhi Gupta et al. (2017) Emperipolesis, entosis and cell cannibalism: Demystifying the cloud. J Oral Maxillofac Pathol. 21(1): 92–98

Nguyen GT, et al. (2017) Neutrophils to the ROScue: Mechanisms of NADPH Oxidase Activation and Bacterial Resistance.Front Cell Infect Microbiol. 7:373.

N. Valade, et al. (2005) Thrombocytosis after trauma: incidence, aetiology, and clinical significance. Br J Anaesth. 94(1):18-23.

Overholtzer M, et al. (2007) A nonapoptotic cell death process, entosis, that occurs by cell-in-cell invasion. Cell. 131(5):966-79.

Ogawa, M. (1993) Differentiation and proliferation of hematopoietic stem cells. Blood, 81, 2844–2853.

O'Brien JJ, et al. (2008) 15-Deoxy-D12,14-PGJ2 enhances platelet production from megakaryocytes. Blood. 112: 4051–4060.

Peng Xia, et al. (2008) Emperipolesis, entosis and beyond: Dance with fate. Cell Res. 18(7):705-7.

Patel, S.R., et.al (2005) Differential roles of microtubule assembly and sliding in proplatelet formation by megakaryocytes. Blood. 106:4076–4085.

Pamuk GE, et al. (2006) Increased circulating platelet-neutrophil, platelet-monocyte complexes, and platelet activation in patients with ulcerative colitis: a comparative study. Am J Hematol. 81(10):753-9.

Polanowska-Grabowska R, et al. (2010) P-selectin-mediated platelet-neutrophil aggregate formation activates neutrophils in mouse and human sickle cell disease. Arterioscler Thromb Vasc Biol 30:2392– 2399

Pinho S, et al. (2018) Lineage-Biased Hematopoietic Stem Cells Are Regulated by Distinct Niches. Dev Cell. 44(5):634-641.e4

Renata Grozovsky, et al. (2015) The Ashwell-Morell receptor regulates hepatic thrombopoietin production via JAK2-STAT3 signaling. Nat Med. 21(1):47-54.

Sungaran R, Markovic B, Chong BH. (1997) Localization and Regulation of Thrombopoietin mRNA Expression in Human Kidney, Liver, Bone Marrow, and Spleen Using In Situ Hybridization. Blood. 89(1):101-7.

Shinguang Qian, et al. (1998) Primary role of the liver in thrombopoietin production shown by tissue-specific knockout. Blood. 92(6):2189-91.

Satoshi Nishimura, et al, (2015) IL-1α induces thrombopoiesis through megakaryocyte rupture in response to acute platelet needs. J Cell Biol. 209(3):453-66

Sayah DM, et al. (2015) Neutrophil extracellular traps are pathogenic in primary graft dysfunction after lung transplantation. Am J Respir Crit Care Med 191:455–463

Schmitt A, et al. (2000) Pathologic interaction between megakaryocytes and polymorphonuclear leukocytes in myelofibrosis. Blood 96(4):1342-7.

Shinjo, K., et al. (1998) Serum thrombopoietin levels in patients correlate inversely with platelet counts during chemotherapy-induced thrombocytopenia. Leukemia. 12:295–300

Shamoto M. (1981) Emperipolesis of hematopoietic cells in myelocytic leukemia. Electron microscopic and phase contrast microscopic studies. Virchows Arch B Cell Pathol Incl Mol Pathol.35(3):283-90.

Solar GP, Kerr WG, Zeigler FC, et al. (1998) Role of c-mpl in early hematopoiesis. Blood. 92:4-10

Sreeramkumar V, et al. (2014) Neutrophils scan for activated platelets to initiate inflammation Science 346:1234-8

Steffen Massberg, et al. (2006) Platelets secrete stromal cell–derived factor 1α and recruit bone marrow–derived progenitor cells to arterial thrombi in vivo. J Exp Med. 203(5): 1221–1233.

Stegner D. et al. (2017) Thrombopoiesis is spatially regulated by the bone marrow vasculature. Nat Commun. 8(1):127

Suratt BT, et al. (2004) Role of the CXCR4/SDF-1 chemokine axis in circulating neutrophil homeostasis. Blood. 104(2):565-71

Shivdasani RA, et al. (1995) Transcription factor NF-E2 is required for platelet formation independent of the actions of thrombopoietin/MGDF in megakaryocyte development. Cell. 81(5):695-704.

Shavit JA, et al.(1998) Impaired megakaryopoiesis and behavioral defects in mafG-null mutant mice. Genes Dev. 12(14):2164-74.

Sandra Pinho, et al. (2018) Lineage-Biased Hematopoietic Stem Cells Are Regulated by Distinct Niches.Dev Cell. 44(5):634-641.e4.

Ton Lisman. (2017). Platelet–neutrophil interactions as drivers of inflammatory and thrombotic disease. Cell Tissue Res.371(3):567-576.

Varun Rastogi, et al. (2014) Emperipolesis – A Review. J Clin Diagn Res. 8(12): ZM01–ZM02.

Vyas P, et al. (1999) Consequences of GATA-1 deficiency in megakaryocytes and platelets. Blood.93(9):2867-75.

Venkateswaran K Iyer, et al. (2009) Variable extent of emperipolesis in the evolution of Rosai Dorfman disease: Diagnostic and pathogenetic implications. J Cytol. 26(3): 111–116.

William B. Slayton, et al. (2002) The spleen is a major site of megakaryopoiesis following transplantation of murine hematopoietic stem cells. Blood. 100:3975-3982

Zarbock A, et al. (2007) Platelet-neutrophil-interactions: linking hemostasis and inflammation. Blood Rev.21(2):99-111.

Zhang L. et al. (2014) A novel role of sphingosine 1-phosphate receptor S1pr1 in mouse thrombopoiesis. J Exp Med. 209(12):2165-81.

Zhang J, et al. (2007) CD41-YFP mice allow in vivo labeling of megakaryocytic cells and reveal a subset of platelets hyperreactive to thrombin stimulation. Exp Hematol. 35(3):490-499.

Zhao M, et al. (2014) Megakaryocytes maintain homeostatic quiescence and promote post-injury regeneration of hematopoietic stem cells. Nat Med. 20(11):1321-6.

Zimmet, J. & Ravid, K. (2000) Polyploidy: occurrence in nature, mechanisms, and significance for the megakaryocyte-platelet system. Experimental Hematology, 28, 3–16. Experimental Hematology, 28, 3–16.

Acknowledgement

First of all, I would like to express my sincere appreciation to my supervisor Prof. Dr. med Steffen Massberg for giving me such a golden opportunity to work in this excellent laboratory and collaborate with many brilliant scientists. Without his help and support, I could not finish my PhD study so successfully.

I also would like to thank my thesis committee members, Prof. Dr. Reinhard Fässler and Prof. Dr. rer. nat. Barbara Walzog. Their insightful suggestions and inspiring discussions always helped me to improve my work.

Similarly, I also would like to thank Dr. med. Tobias Petzold and show my deepest respect to him. As my direct supervisor, he not only gave me an interesting project, more importantly, he taught me how to work as a good scientist. It was always a pleasure (and an honor) to work in AG Petzold where I met my best friends in Germany, Inas Saleh, Verena Warm, Manuela Thienel, Jan Strecker, Christian Weber, Elisabeth Raatz, Enzo Lüsebrink and Cuong Kieu. Your friendly help and love made my life and work much easier in Germany.

I also very appreciate the help and support from Michael Lorenz, Hellen Ishikawa-Ankerhold and Susanne Sauer, which make me overcome many problems in my project.

At last, I would like to thank my parents and Weijing Ge, your love and support are the greatest impetus for me to work in the scientific filed. Thank you very much, I love you all.